



# Microstratigraphic analysis of the main Roman road in *Hispania*: the *Via Augusta* where it passes through the *Ianus Augustus* (Mengíbar, Spain)

Mario Gutiérrez-Rodríguez<sup>1,2</sup> · Miguel Ángel Lechuga Chica<sup>1</sup> · María Isabel Moreno Padilla<sup>1</sup> · Juan Pedro Bellón Ruiz<sup>1</sup>

Received: 21 September 2020 / Accepted: 9 June 2022 / Published online: 4 July 2022  
© The Author(s) 2022

## Abstract

Roman roads are omnipresent in the Mediterranean basin. Despite the methodological advances achieved, interdisciplinary studies including geoarchaeological techniques are still rare. The aim of this study is to offer a microstratigraphic analysis of an important Roman road in order to characterise the raw materials and construction techniques used to build it and their evolution over time. Our research focuses on the *Via Augusta*, the longest road in Roman *Hispania*, where it passes through the *Ianus Augustus* (Mengíbar, Spain), a monumental complex on the frontier between the provinces of *Baetica* and *Tarraconensis*. Archaeological excavations of this road have revealed vertical stratigraphic variations, suggesting the presence of several transit surfaces and repair works. A protocol was designed to characterise the road deposits at the microscale, where micromorphology revealed six overlying roads and their construction techniques. The combination of micromorphology,  $\mu$ -XRF and the study of the textural parameters of the deposits allowed us to identify the raw materials used and their sources, as well as the specific features generated during the construction and use of the road. The results show how the technical solutions used survived as a tradition for centuries, and how the repair works identified in the stratigraphic sequence have a correlation with the road maintenance works mentioned in the Roman epigraphic record of *Hispania Baetica*. This study shows how detailed microstratigraphic analyses of Roman roads are very effective in the characterisation of road biographies.

**Keywords** Roman road · *Via Augusta* · GIS · Geoarchaeology · Micromorphology

## Introduction

The Roman Empire was made up of a myriad of towns and territories (*civitates*) that were linked by an impressive road system. This road network was a true emblem of Roman civilisation that allowed new territories to be conquered and trade to be developed. It also symbolised political power, connected people and allowed the rapid spread of new ideas across a geographical area that was larger than modern-day Europe. As a result, these infrastructures conform to a vast archaeological heritage in the Mediterranean basin with an important research background (Sillières 1990; Chevalier 1997). In this respect, studies have traditionally explored the role of Roman roads in ancient topography (Gautier 1769; Albenga 1918; Fustier 1960; Forbes 1964; Radke 1981; Quilici and Quilici 1992; Kolb 2019), especially regarding Roman rural field systems (*centuriationes*) (Chouquer and Favory 1991; Botazzi 1992; Ciampoltrini and Andreotti 1994; Ariño Gil et al. 2004); the relationship between roads

---

✉ Mario Gutiérrez-Rodríguez  
mgrodrig@ujaen.es

Miguel Ángel Lechuga Chica  
mlechuga@ujaen.es

María Isabel Moreno Padilla  
imoreno@ujaen.es

Juan Pedro Bellón Ruiz  
jbellon@ujaen.es

<sup>1</sup> Instituto Universitario de Investigación en Arqueología Ibérica, University of Jaén, Campus Las Lagunillas, 23071 Jaén, Spain

<sup>2</sup> School of Archaeology and Ancient History, University of Leicester, Mayor's Walk, Leicester LE1 7RH, UK

and the urban necropolises and the entrances to the towns (Schattner and Ruipérez 2010) and their association with overland trade (Batino et al. 1999; Berechman 2003; Hitchner 2012; Orengo and Livarda 2016). With regard to the roads as part of Roman material culture, research has generally emphasised the analysis of their construction techniques (Forbes 1964; Quilici 1992; Quilici and Quilici 1992; Rosada 1992; Xeidakis and Varagouli 1997; Moreno Gallo 2004), geotechnical properties (Garilli et al. 2017) and the modern restoration of ancient routes (Petrucci 2013). In this respect, the growing interest in the surveying (Sidebotham et al. 2000; Magli et al. 2014) and stratigraphic excavation (Quilici and Quilici 1992; Moreno Gallo 2004; Garilli et al. 2017) of Roman roads has been a crucial milestone. In recent decades, the application of new analytical methods to the Roman road research agenda has been significant, with the progressive generalisation of aerial photography and photogrammetry (Gasparini et al. 2019), remote sensing (Keay et al. 2014), geophysics (Bernardini et al. 2018) and spatial analysis (Evangelidis et al. 2015; Güimil-Fariña and Parcero-Oubiña 2015; Verbrugge et al. 2017).

Nevertheless, and despite this methodological development and an increasing number of excavations on roads across the Roman Empire, a misconstrued idea of the paradigmatic structure and construction techniques of a standard Roman road has been widespread until fairly recently. A long tradition of studies (Chevallier 1997; Moreno Gallo 2004; Sillières, 1990, amongst others) consolidated the idea that Roman roads consist of a characteristic succession of layers from bottom to top: the basement or *statumen* (boulders), the *rudus* (gravel and coarse sand), the *nucleus* (crushed stones, sand and mortar/clay) and, finally, the *summa cresta* or *pavimentum* (stone slabs). However, the information given in the classical texts does not correspond to this logical sequence and the archaeological evidence is much more diverse than that simple scheme. Furthermore, ancient texts referring to Roman roads are scarce and do not mention such a terminology and succession of layers (Rodríguez Morales 2011). Moreover, stone-paved roads (*viae lapidae stratae*), such as the *Via Appia*, were considered by classical authors to be exceptions (Status, *Silvae*, 2, 2, 12; Procopius, *History of the Wars*, V, 14, 6–10), whilst those made with gravel (*viae glarea iniectae*) or just by conditioning and trampling the soil (*viae terrenae*), following the terminology used by Ulpianus (*Digesto*, 43, 11, 1, 2), were more frequent (Plutarch, *Parallel Lives, Gaius Gracchus*, 7; Status, *Silvae*, 4, 3). In fact, apart from the well-known text of Status (*Silvae*, 4, 3), the few references in classical texts on how to build roads explicitly mention the use of gravel and not slabs to pave them. This is the case of Tibullus and Plutarch, who stated that “the roads were made in a straight line, right through the country, partly of quarried stone and partly with tight-rammed masses of earth” (Plutarch, *Parallel Lives, Gaius*

*Gracchus*, 7) and “see, winding upward through the Latin land/ Yon highway past, the Alban citadel/ At great Messala’s mandate made/ In fitted stones and firm-set gravel laid/ Thy monument forever more to stand!” (Tibullus, 1, 7, 57). Besides, excavations of Roman roads across the different provinces of the former Roman Empire reveal a considerable stratigraphic variability in terms of their construction techniques, raw materials and composition, due to the possibilities and limitations of the local geology and the repairs carried out over time (Quilici and Quilici 1992; Xeidakis and Varagouli 1997; Moreno Gallo 2004; Garilli et al. 2017; Charbonnier and Cammas 2018, amongst others). These excavations also document a predominance of multiple gravel deposits, which sometimes represent not just one, but a sequence of several overlying roads. The aforementioned terminological misinterpretation comes from a misreading of N. Bergier’s *Histoire des Grandes Chemins de l’Empire Romain* (1622), which is considered to be the starting point for Roman road research (Rodríguez Morales 2010). Subsequent scholars mistakenly identified and erroneously translated the terms Bergier used to describe the different stratigraphic units identified in his excavations carried out in the seventeenth century.

Even Bergier, in his pioneering work, suggested that methodologically further research should focus attention on “the materials found in different layers [of the roads], their order assigning each one a name, and making them distinguishable” (free translation of Bergier 1622, p. 142). Despite this having been one of the main aims on the research of Roman roads, the deposits have normally been poorly described from a geoarchaeological perspective. As roads consist of gravel and sand deposits, geoarchaeology has the potential to contribute significant data to the recognition of site preparation work prior to the road construction, as well as to the identification and characterisation of the raw materials used and where they were sourced from. It can also offer information on the building techniques used, the identification of transited surfaces, possible differences and similarities in the case of road sequences and periods of abandonment and disuse. However, detailed geoarchaeological analyses of road and traffic deposits are not common in Roman road literature. In this respect, and without the aim of carrying out a systematic review of the subject, we can highlight the study by Capedri et al. (2003) of the petrographic and geochemical characterisation of stone-paved roads on the Po plain and the identification of raw material source areas. Garilli et al. (2017) offer a detailed stratigraphic and geotechnical characterisation of the gravel deposits of nine prominent Roman roads in Italy, Greece and southern France. There also are some micromorphology studies of roads and traffic deposits (Cammass and Watez 2009, p. 209; Charbonnier and Cammas 2015, 2018; Gebhardt and Langohr 2015). Amongst them, those of Charbonnier and

Cammas (Charbonnier and Cammas 2015, 2018) on the micromorphology of Roman road deposits in urban environments in northern France stand out. They undertook a microfacies analysis of road, street and lane contexts, identifying specific and significant facies and features related to their construction, maintenance, periods of use and abandonment. These studies illustrate the significant contribution of geoarchaeology to the understanding of Roman roads and how much of this information is contained at the microscale.

The aim of this study is to carry out a microstratigraphic analysis of an outstanding Roman road in *Hispania*. Our specific objectives are the identification of features related with the construction of the road, the characterisation of the different materials and their sources in the landscape as well as the construction techniques employed and, finally, the identification of maintenance and repair works. The premise of this study is that, when considered together, the different questions mentioned above and the implementation of microstratigraphic techniques of analysis could offer a very detailed view of the diachronic evolution of a Roman road in a biographic sense (we understand the biographic perspective in the sense proposed by Wouters 2020). Specifically, our research focuses on the *Via Augusta*, the longest road in Roman *Hispania* (Fig. 1). This paper looks specifically at the area where the *Via Augusta* passes through a singular landmark in the ancient geography: the *Ianus Augustus* (Mengíbar, Spain), a monumental complex on the frontier between the provinces of *Hispania Baetica* and *Hispania Tarraconensis* (Figs. 1, 2 and 4). The excavation of the *Via Augusta* at this point of its layout offered a complex stratigraphic sequence composed of gravel deposits on the local natural soil (Fig. 6).

## The geological and archaeological context of the *Via Augusta* where it passes through the *Ianus Augustus*

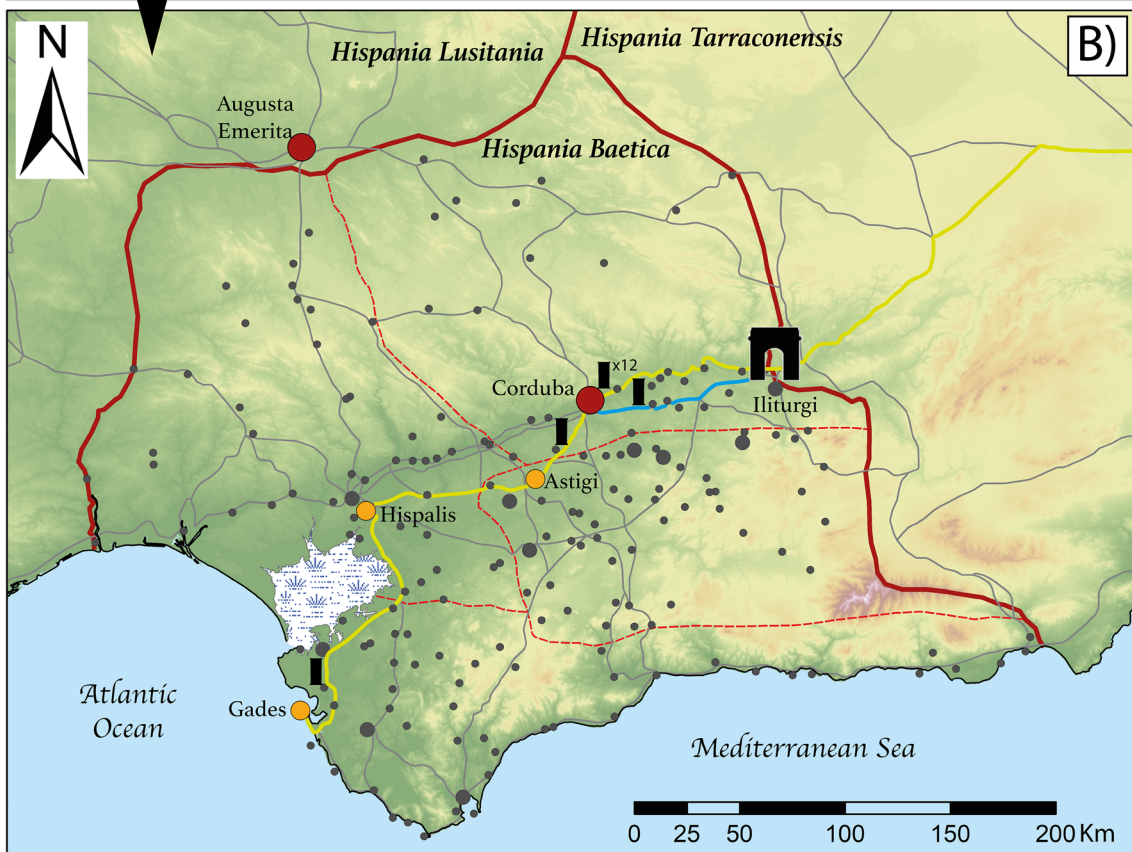
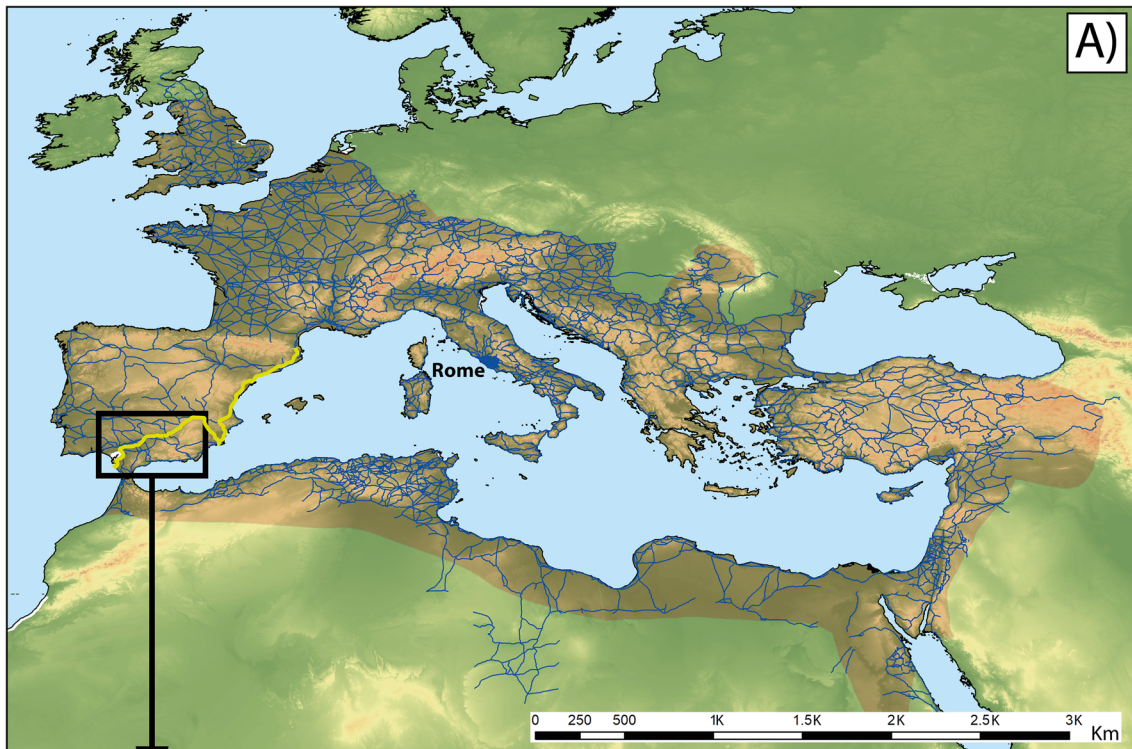
### Geographical and geological setting

The site is set in the north-eastern sector of the Guadalquivir basin (Fig. 3A), a foreland basin formed between the Iberian Massif to the north and the Betic Cordillera to the south. It is one of the largest Tertiary basins on the Iberian Peninsula. It is bordered by the Hercynian basement of the Sierra Morena to the north (comprising a wide range of Palaeozoic plutonic and metamorphic rocks, such as granites, slates, schists and hornfels); to the south by the Subetic Domain of the External Zone of the Betic Cordillera (Sierra Mágina, comprising mainly Mesozoic limestones) and, to the east, by the Prebetic Domain of the External Zone of the Betic Cordillera (Sierra de Cazorla, composed of Mesozoic carbonate lithologies). This Tertiary basin is crossed by the course of

the River Guadalquivir that cuts through its marine sedimentary infill, which comprises several lithostratigraphic units ranging from the Middle Miocene to the Pliocene. Except for the Olistostromic Serravallian unit, which is composed of clays, red sandstones, gypsum and dolostones, the rest of the units consist of marls, bioclastic limestones, calcarenites and sandstones with carbonate cement (Jimenez-Espinosa et al. 2016). It is in these last units that our study area is located.

The local geology (Fig. 3B) is a determining factor for our understanding of the materials used in the construction of the Roman road, as well as for the technical solutions adopted. The landscape around the site is defined by a smooth orography of rounded hills (with a maximum difference in elevation of less than 500 m) and by the course of the River Guadalquivir and its tributaries, the Guadalbullón and the Guadiel, which make up a hydrological network that flows westward. The oldest geological materials date from the Upper Miocene, when the end of this basin segment was filled. Specifically, it is the Porcuna Unit (Fig. 3B: 1), which has a tabular morphology and is composed of marls that are yellowish-grey on the surface and greyish-bluish where freshly cut. These marls present a mineral fraction composed of a very well-sorted fine to medium sand, in which abundant lamellibranchs and rounded quartz stand out (ITGE 1990a, b). On the roof of the unit, there is a series of silt, bioclastic sandstones and calcarenite layers interfingering with marls. The baseline contact of this unit is not clear due to the continuous disturbance by agriculture, although as it is on various units and facies of diverse chronology, it can be concluded that it constitutes a discordance in the regional geology. A conglomerate unit that also belongs chronologically to the Miocene (Fig. 3) appears discordantly on the Porcuna Unit in isolated outcrops, especially to the east of the River Guadalbullón. It shows a cyclic sequence of conglomerates with sporadic levels of white marls and silt, changing to rosaceous tones towards the roof of the sequence. The clasts are mainly calcareous, although other lithologies are present.

Other lithological units present in the surroundings of the *Via Augusta* where it passes through the *Ianus Augustus* are the alluvial Quaternary deposits of the Guadalquivir and Guadalbullón river terraces (Fig. 3B: 3–5) that unconformably overlie the Mio-Pliocene lithological units (ITGE 1990a, b). The thickness of these alluvial deposits ranges from 5 to 12 m along the basin. Although three terraces are identified in the Guadalquivir basin, only two of them—the middle and the lower—are present in the study area. The upper terrace is very eroded and it can only be found a few kilometres east to the study area. These terraces are composed of silt and gravel deposits, sometimes cemented, and red clay deposits are scarce. The middle terrace is the most extensive of the three and is c. 50 m below the relicts of the upper terrace. It shows a fining-upward megasequence with a complex



- Provincial capital
- Conventual capital
- Coloniae
- Municipia
- Lacus Ligustinus
- Roman roads
- Provincial boundaries
- Conventual boundaries
- Ianus Augustus
- Milestones mentioning the Ianus Augustus or repairs along the Via Augusta
- Via Augusta (main route)
- Via Augusta (alternative route, or Alio itinere)

**Fig. 1** Contextualization of the *Via Augusta*. **A** The *Via Augusta* (yellow line) within the road network of the Roman Empire at its maximum extent in 117 AD (orange shading). **B** *Via Augusta* layout in *Baetica* province, showing the location of the *Ianus Augustus* on the border between the provinces of *Baetica* and *Tarraconensis*, as well as the milestones and epigraphs that explicitly mention the *Ianus Augustus* or repairs along the *Via Augusta*

internal structure that, in broad terms, can be grouped into channel facies at the bottom of the sequence, and floodplain facies in the upper part (ITGE 1990a, b; Lorite-Herrera et al. 2008; Jimenez-Espinosa et al. 2016). This terrace has been dated by Baena (1993) to 80 k years BP.

Finally, recent alluvial deposits are also present on the course of the Rivers Guadalquivir, Guadalbullón and Guadiel (Fig. 3B: 6), as well as colluvial deposits of glaciis in the vicinity (Fig. 3B: 7), configuring a concave morphology of the landscape. The lithology of these deposits is composed of silts and marls and their genesis is dominated by solifluction processes.

In terms of soils, the identified section of the *Via Augusta* rests on a calcic Luvisol that is notable for the absence of coarse components and gravels. These clay-rich soils, which are typical of plains and low slopes in Mediterranean-climate areas, are well-represented in the study area. Beneath the gravel deposits that make up the *Via Augusta*, two soil horizons, A (surface layer) and Bk (subsurface layer: a clay deposit with secondary calcium carbonate accumulations forming carbonate crusts and nodules), were identified, whilst soil horizons C (transitional layer) and R (contact with the bedrock) are located at a greater depth than the excavated area.

### The *Ianus Augustus* monumental complex

The *Via Augusta* was built between 8 and 2 BC. More than 1500 km long, this *via militaris* of extraordinary strategic importance (Sillières 1981) runs from *Gades* (Cádiz, Spain) to the Pyrenees, where it connects with the *Via Domitia* and, ultimately, with Rome itself, as shown on the Vicarello Cups and in the Antonine Itinerary (Sillières 1990; Roldán Hervás and Caballero Casado 2014). The analysed section of the *Via Augusta* runs through the *Ianus Augustus* monumental complex (Fig. 4). The provincial organisation designed by Augustus entailed the creation of the senatorial province of *Baetica* in 27 BC (España Chamorro 2021). The establishment of an interprovincial frontier between *Baetica* and the imperial province of *Tarraconensis* involved establishing a landmark that would act as a physical and a visual limit and be conceived as a starting point (*caput viae*) of the Roman Empire's communication networks in this area (Sillières 1994; España-Chamorro 2017; Bellón Ruiz et al. 2021). This *caput viae*, which was named *Ianus Augustus* in honour of its founder, is only referenced on the Baetican

milestones and in the honorific epigraphy. The *Ianus* was the starting point for the whole of the *Via Augusta* in province, as confirmed by several milestones dating from Augustan to Flavian times (Figs. 1 and 4). The road, the *Ianus Augustus* and the River *Baetis*, constituted the most significant and powerful elements to delimit this new administrative territory monumentally and symbolically (Sillières 1994; España-Chamorro 2017; Bellón Ruiz et al. 2021). The *Via Augusta* would have acted as the backbone and unifying element in the Baetic territory (España-Chamorro 2017). The *Ianus Augustus* monumental complex would therefore have acquired an important political and economic role in the Roman imperial structure of the region. It was a symbol of the power of Rome and Augustus and, moreover, a paradigm of Augustan imperial propaganda with regard to the mechanisms of territorial integration and ideological control through a very select scenography that marked the most important geographical points of the Empire (Guédon 2018).

Despite several attempts to find it using epigraphic sources (Hübner 1888; Blázquez 1914; Sillières 1981, 1994; Schmidt 2018), its location was archaeologically unknown. Between 2018 and 2019, we carried out interdisciplinary research in the area proposed by the abovementioned previous studies, as the most possible location of the *Ianus Augustus* remains (Fig. 1B). Our survey and excavation work made it possible to archaeologically locate this monument and to define the remaining elements associated with the different dimensions of the *Ianus* (Bellón Ruiz et al. 2021). Our excavations show that the main element of this complex was an arch (of which only its *opus caementicium* foundations are preserved) (Fig. 4) with architectural decoration and sculptural elements, including gilded bronze fragments possibly associated with a sculptural group that would have crowned the arch. Also, a monumental structure was documented next to the arch, although only the ground plan of sandstone blocks on a thick foundation of *opus caementicium* is preserved (Fig. 4). Like the arch, this structure was intentionally dismantled and plundered. As shown by pottery and numismatic finds, this dismantling took place in Late Antiquity, in the second quarter of the fourth century AD (Bellón Ruiz et al. 2021). Next to this ashlar structure, in a pit associated with the plundering of the structure, architectural elements from the unpreserved upper part of the monument were documented. Of particular note amongst them were decorated cornice fragments and a large fragment of monumental *pulvinus* (a decorative element of the top part of an altar). This building has been interpreted as a possible *ara terminalis*, or a monumental altar associated with the imperial cult and rites of passage, given that the *Ianus* itself represented a landmark: the gates to *Baetica* province (Bellón Ruiz et al. 2021).

Finally, to the east of the complex and next to the River *Baetis*, on a level some 20 m below the arch and altar, the

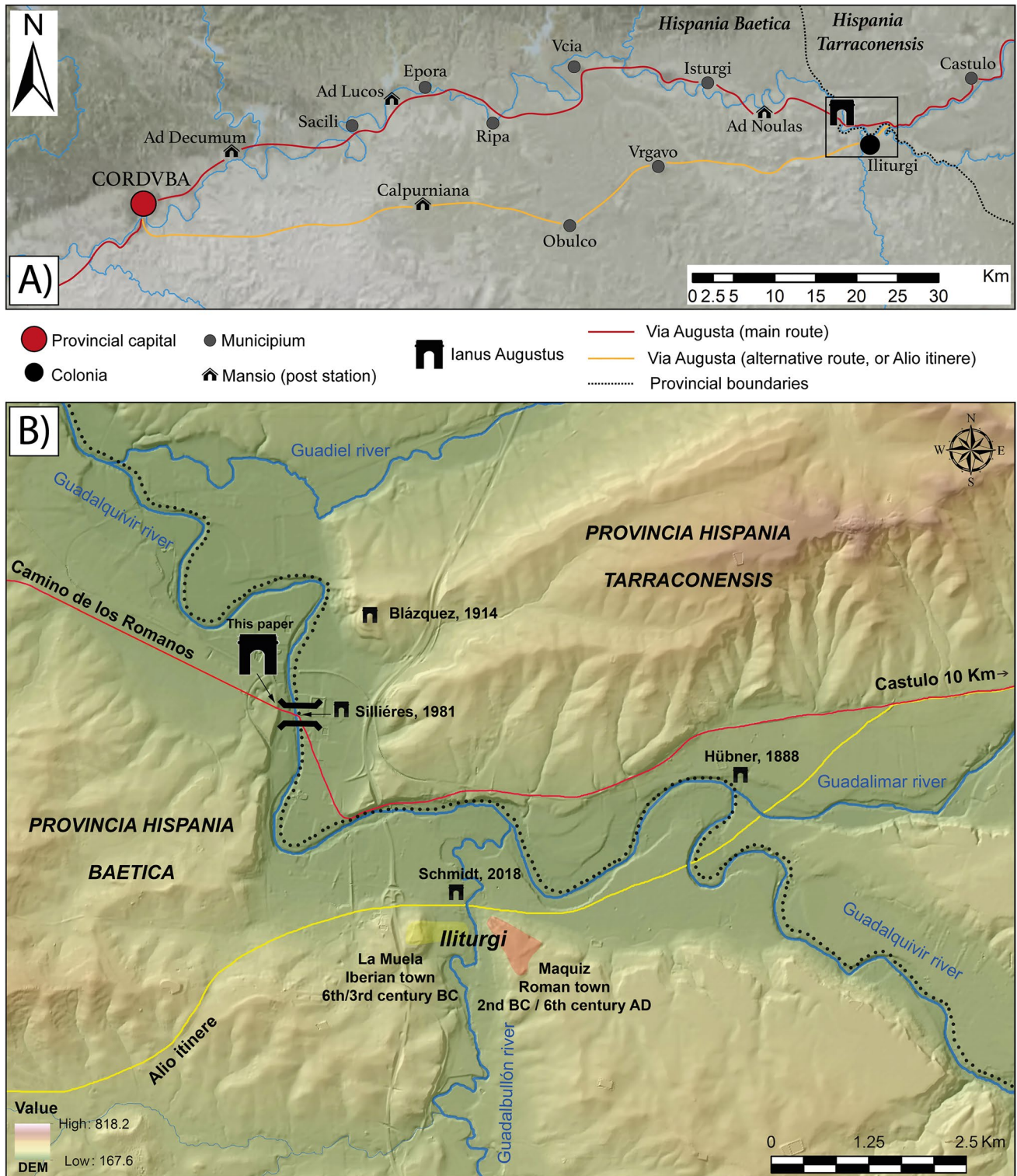


**Fig. 2** Via Augusta layout. **A** Via Augusta layout from Corduba to Castulo, showing its main and the secondary routes and the location of the Janus Augustus. **B** Location of the Via Augusta and the Janus Augustus in the surroundings of the Roman town of Illiturgi

(Mengíbar, Jaén, Spain), showing the Via Augusta layout (both its main and secondary route) and different hypotheses regarding the location of the Janus Augustus in previous literature

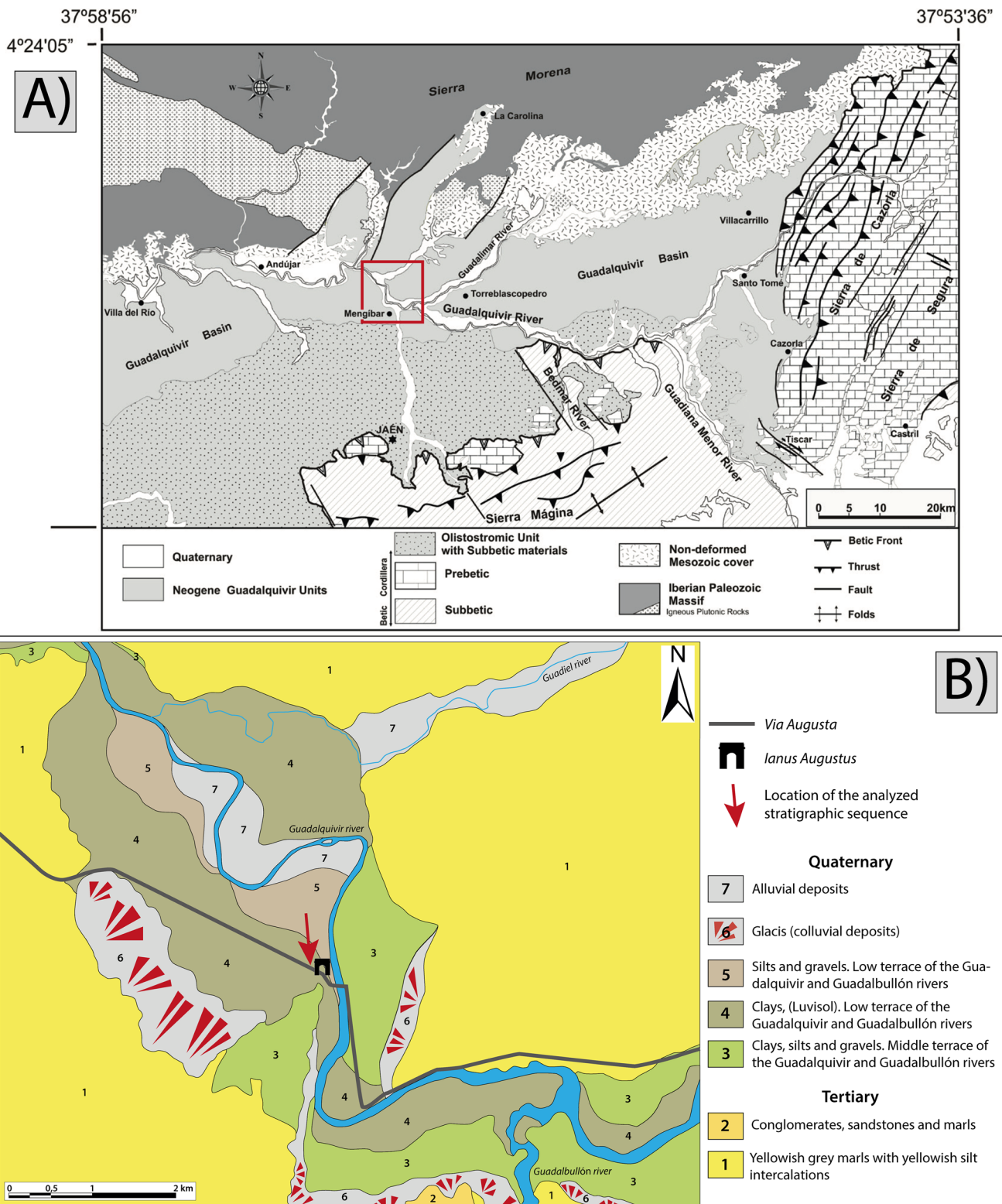


**Fig. 3** Location of the *Via Augusta* where it passes through the *Ianus Augustus*. **A** Regional geology (modified from Lorite-Herrera et al. 2008: 2042). **B** Local geology and lithologies (cartographic base modified from the MAGNA series, Instituto Geológico y Minero de España)



**Fig. 4** Excavation area of the *Ianus Augustus* monumental complex. **A** Aerial view indicating three of the sondages. In red, the *Via Augusta* where it passes through the foundations of the arch pillars. **B** Orthophotography and local relief model of the Roman road: the

red line in the sondage indicates the studied profile. Note the sondage on the pillars of the monumental arch and the Roman road, and the monumental altar next to the arch



micro-survey defined an archaeological area approaching 1 hectare in size. It contained abundant finds, including *tegula* fragments, building material, ashlar and pottery, particularly Hispanic *terra sigillata* (Bellón Ruiz et al. 2021). The geophysical survey showed significant anomalies that made it possible to delimit several buildings facing the *Via Augusta*, which could possibly have been associated with administrative and service tasks. From this point, the road would have been subject to the unevenness of the terrain, at the same time as it would have been part of the scenographic design. The ascent to the *Ianus Augustus* would have framed and emphasised its monumentality, on a route that symbolised not only the passage from one province to another, but also the power of the emperor, through an element as evocative as the gate guarded by the god *Ianus* (Bellón Ruiz et al. 2021; Sillières 1994).

Of all these elements, we focus in this paper on the *Via Augusta*. This road is recurrently mentioned in the regional historical cartography. An extensive collection of place names related with the road shows the permanency of this ancient path in collective memory and the landscapes through time. Historical cartography associates the placename “Camino de los romanos” or “Roman’s road” to this feature at least from the eighteenth century. This led other researchers to identify this path with a Roman road (Sillières 1990; Corzo Sánchez and Toscano San Gil 1992; Melchor Gil 1994). However, since the tenth century on, Mediaeval literary sources refer to this path as “Arrecife”, an Arabism derived from “al-raṣīf” meaning ‘the paved stone’ and “the road” (Franco-Sánchez 2017). In this sense, Muslims usually called paved or cobbled roads “Arrecife” (Torres Balbás 1959). The road is mentioned in a historic episode, when Abd al Rahman III and his army set up their camp at the site of “al Haniya” (“the arch”) on their march from Córdoba to the north of the Iberian Peninsula in 912 AD (Zanón 1986). After identifying the road in historical documents, we developed a survey by means of UAV and photogrammetry. We were able to verify that this ancient road was preserved 2.5 km long with an average width of 7 m and a height of 1.6 m above the surrounding terrain, following a straight SE-NW orientation (Fig. 5A–C). This section has irregular masonry remains delimiting its width (*margines*) (Fig. 5D) and passes through the pillars of the *Ianus Augustus* arch.

We carried out a stratigraphic sondage where the road passes through the arch. The excavation of the road revealed a complex stratigraphic sequence (Bellón Ruiz et al. 2021) composed of overlying thick gravel beds with evidence of trampling and compaction (Fig. 6). In this regard, the horizontal tendency of the clasts is noteworthy. A common characteristic of all the deposits that make up the road is their lithological and granulometric

composition, which is defined by the presence of mainly limestone, dolomite, slate and quartzite gravels. However, there are granulometric differences amongst these gravel layers, as well as in terms of the accommodation and absence/presence of fine mineral material. Most of the gravel layers are massive and very thick (12 to 38 cm), with a significant absence of fine material (Fig. 6A–B: stratigraphic units 3, 4, 6, 8, 9, 10 and 13). In contrast, some deposits are thinner (2–4 cm) with smaller gravel clasts, which are supported in a sandy clay matrix (Fig. 6A–B: stratigraphic units 5, 7 and 12). Although most of the identified deposits are homometric and the coarse fraction has a heterogeneous distribution, locally they can show reverse grading (Fig. 6C). This sequence is truncated and eroded on its upper part. The starting hypothesis of this study is that the thinner layers with clayey matrix are traffic transit surfaces, whilst the massive, thick gravel deposits correspond to construction infillings, or preparation layers for the road surfaces.

## Materials and methods

### Archaeological soil and sediment micromorphology

Undisturbed and oriented soil and sediment micromorphology samples were collected from stratigraphic profiles produced during the 2018 excavation season. Sampling strategy was systematic, covering all the stratigraphic units identified in the field (Fig. 6). Blocks stabilised with plaster of Paris bandages were later oven-dried for 1 day at 50 °C. Impregnation was carried out under vacuum with polyester resin (Palatal P4-01), styrene monomer and MEK catalyst. A total of 18 thin sections were studied. They were analysed under plane-polarised (PPL), cross-polarised (XPL) and oblique incident (OIL) lights. Descriptive standard criteria were followed (Courty et al. 1989; Stoops 2003; Stoops et al. 2010; Karkanis and Goldberg 2019), paying particular attention to specific features previously reported in similar contexts in which micromorphology was used (Gé et al. 1993; Rentzel et al. 2017; Charbonnier and Cammas 2018).

Here, we use the microfacies concept in the sense of Flügel to refer to the arrangement of sedimentary constituents by distinct and recurrent groups of similar composition and organisation within a particular thin section (Flügel 2004). Thus, through microfacies analysis, it was possible to group similar characteristics of lithological composition, geometric association and post-depositional changes, thus allowing us to recognise patterns in different thin sections. This is based on the principle that distinct events, depositional environments and post-depositional processes produce a particular set of

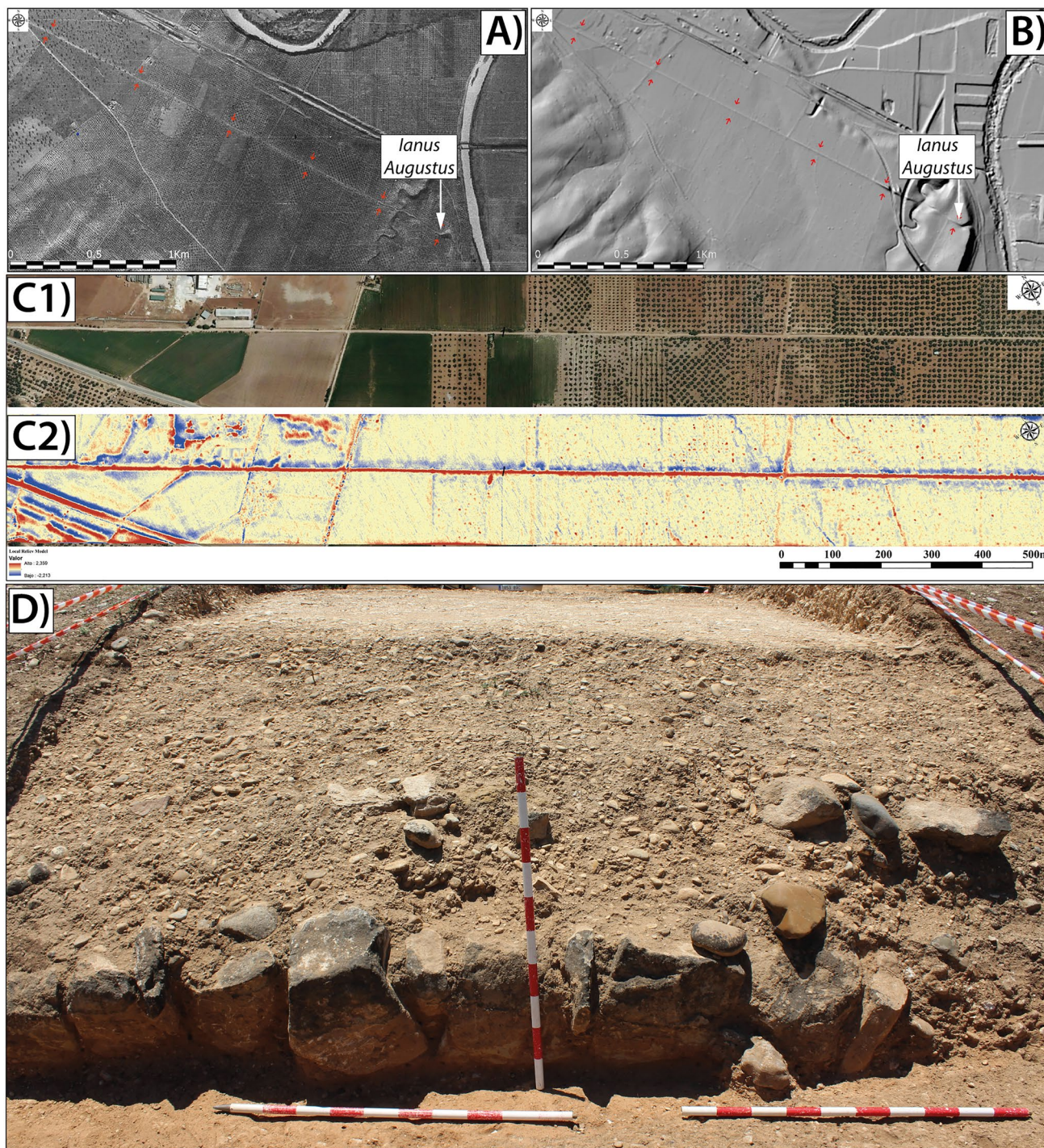


**Fig. 5** The *Via Augusta* layout: **A** Orthophotography of the American Flight Series B (1956) and **B** MDT Hillsade show the preserved 2.5 km of the *Via Augusta* layout, its straight SE-NW orientation and the location of the *Ianus Augustus*; **C1** detail orthophotography and **C2** local relief model highlight the *Via Augusta* average height

of 1.6 m above the surrounding terrain. Derivate of LIDAR-PNOA 2008–2015 CC-BY scne.es; **D** photograph of the *margines* (stone margins) delimiting the Roman road in one of the sondages carried out

microfacies units that, in turn, can be associated with a specific microfacies type (Courty 2001; Flügel 2004; Goldberg et al. 2009).

Regarding sampling and micromorphological documentation, the site was included in a global reference system (UTM ETRS89-30 N) using a total station. Photographic

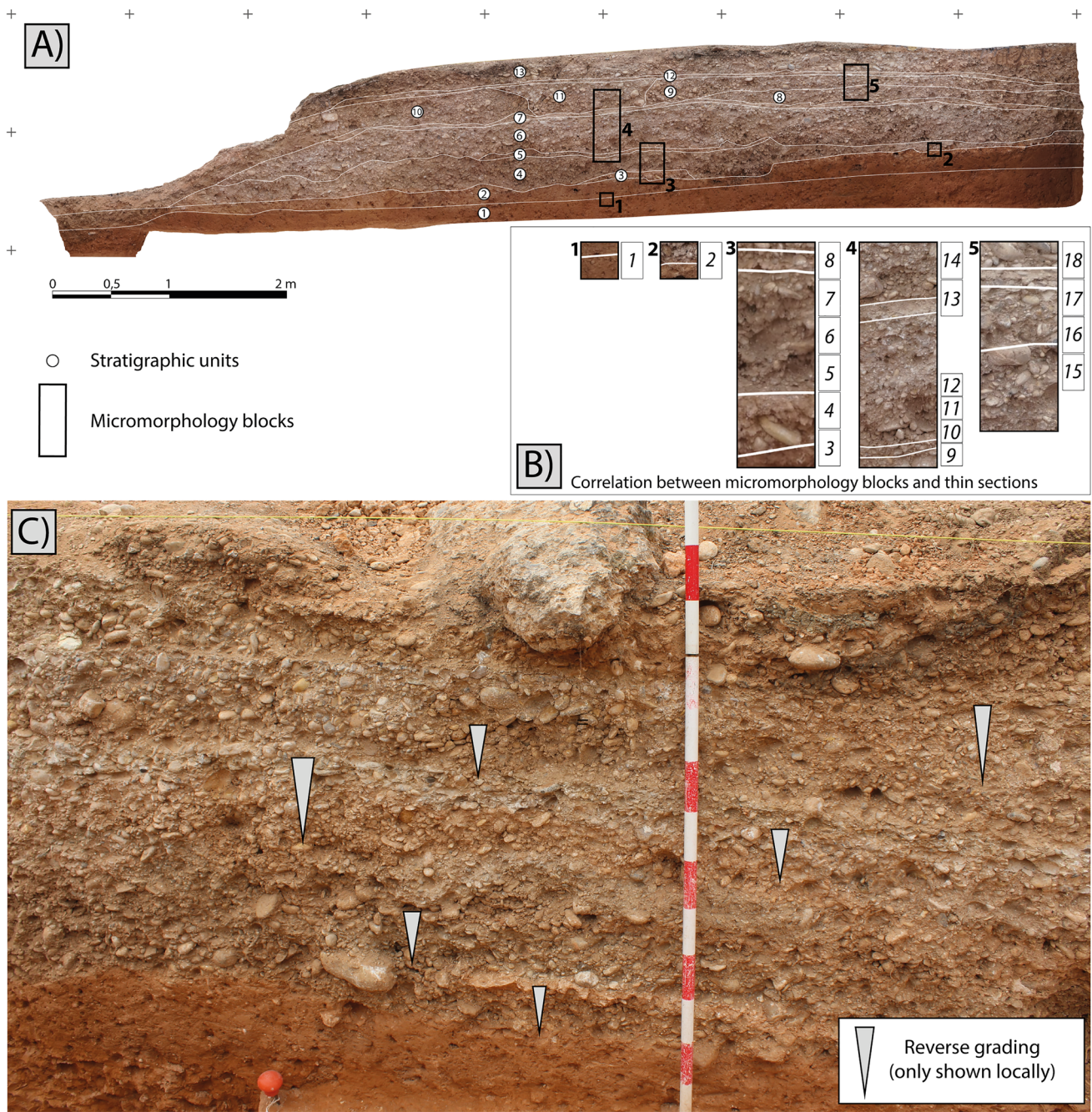


**Fig. 6** Stratigraphy and sampling of the *Via Augusta*. **A** Stratigraphic sequence indicating the different stratigraphic units and the location of micromorphology blocks; **B** correlation between micromorphol-

ogy blocks and thin sections (henceforth samples); **C** detail of the profile indicating the heterogeneous distribution of the gravels that locally show reverse grading

data from the profiles was collected with a Canon 750D, using control points to provide scale and orientation to the 3D modelling according to the local coordinates system. SfM technology (commercial software, Agisoft Photoscan) was used to produce volumetric models from the photographs. The studied thin sections were scanned by using

MWSI (Gutiérrez-Rodríguez et al. 2018). This technique acquires the image directly from the microscope through a camera and Microvisioneer desktop software (<http://www.microvisioneer.com/>). The obtained high-resolution thin section scans were used for the study of textural parameters of the deposits through image analysis and segmentation.

## Image analysis and segmentation

High-resolution scans of the thin sections were analysed with JMicroVision 1.3.3 software (Roduit 2007) in order to explore:

1. Percentages of porosity, grains—sand and gravel fractions—and micromass understood as the fine material of the deposits composed of clay, fine silt and coarse silt (Stoops 2003, p. 93; Stoops and Mees 2018, pp. 74–75).
2. Textural parameters of the grain fraction, specifically: area, orientation, compactness, equivalent circular diameter and elongation (Table 1).
3. Percentages of the different lithologies used in the road building.

These percentages and parameters were characterised for each of the different microfacies identified in the micromorphology. For porosity, grains and micromass characterisation, several filters regarding morphology (closing, erosion, opening) and enhancement (background extraction) were applied to the high-resolution scans after thresholding. This allowed an enhanced segmentation of the different features (voids, grains and micromass). Once the grains had been segmented and extracted, the studied parameters (Table 1) were analysed using frequency histograms. The different lithologies were determined by point counting. The number of points (600) was estimated by observing the evolution plot that shows the variation in the measured percentages. Thus, the point counting is statistically significant when the ratio of each component remains constant, in our case, the ratios of the different lithologies. In contrast to traditional grain-size and textural analyses, this protocol explores these variables in their microstratigraphic context and on a microscopic scale of analysis, something impossible to achieve in a traditional bulk sediment sampling.

## μ-XRF

Elemental composition of the thin sections was explored through μ-XRF. The analyses were conducted with a Horiba XGT-7000 μ-XRF spectrometer housed in the School of Archaeology and Ancient History, University of Leicester. Measurements were taken under full vacuum conditions. This spectrometer was equipped with a microfocus X-ray tube with an Rh anode, a monocapillary lens for X-ray focusing and a Peltier cooled Silicon Drift Detector (SDD) calibrated to Kα1 line. The sample chamber (300 × 300 × 80 mm) incorporated an XYZ motorised stage for sample positioning. A high-resolution microscope was used to position the sample at the desired distance from the monocapillary. To increase the sensitivity of the low Z elements, the sample chamber was brought under vacuum. For the mapping analysis of the samples, a spot size of 100 μm was chosen at an operating X-ray tube voltage of 50 kV, an acquisition time of 2000s, a process time of 6 and a current of 1 mA. Mappings and concentration values were obtained with INCA software (Version 5.05).

## Results

### Archaeological soil micromorphology and μ-XRF

#### Microfacies analysis

A total of 3 microfacies types with 9 subtypes were identified in the thin sections: the Luvisol substrate, traffic surfaces and gravel deposits as constructive infills.

The most discriminating factors in defining gravel microfacies were granulometric differences between the deposits, the degree of accommodation and the absence/

**Table 1** Textural parameters of the grain fraction analysed with JMicroVision 1.3.3

Parameter	Description	Computation	References
Area	Area of the grain. Possible holes within grains are not counted	Sum of at least 8-related pixels	(Roduit 2007, p. 65)
Orientation	An angle of 0–180°, defined in the trigonometric direction between the horizontal axis and the major axis of the ellipse calculated from the moments of inertia	$\text{Orientation} = \frac{180}{2\pi} \tan^{-1} \left[ \frac{2\mu_{11}}{\mu_{20} - \mu_{02}} \right]$	(Roduit 2007, p. 69)
Compactness	A factor indicating the degree of compactness of the object. The area and the perimeter are two parameters invariant to translation and rotation. Dividing the area by the square of the perimeter cancels the unit of measurement and, therefore, an invariance at the change of scale is obtained. The $4\pi$ normalises the compactness value to 1 for a sphere	$\text{Compactness} = \frac{4\pi * \text{Area}}{(\text{Perimeter})^2}$	(Roduit 2007, p. 69)
Equivalent circular diameter	The diameter of a circle with an area identical to that of the object	$\text{Equivalentcirculardiameter} = \sqrt{\frac{4 * \text{Area}}{\pi}}$	(Roduit 2007, p. 69)
Elongation	Elongation of the grains, which can be expressed by the length to width ratio. Roduit's formula gives values of between 0 and 1	$\text{Elongation} = \frac{\text{Length}}{\text{Width}}$	(Roduit 2007, p. 70)

presence of fine material. They are composed of dumped and trampled detritic materials and 5 subtypes were identified. In contrast, traffic surfaces show a higher amount of fine material composed of carbonate clay, which is not present in the geological substrate of the *Via Augusta* layout. The spatial distribution of the microfacies types identified (Table 2) helped to unravel the road sequence and allowed the identification of 6 different overlapping roads (Fig. 9):

**Road 1** This is the most complex of the identified roads in terms of compositional variances and stratigraphy, since it alternates gravel deposits and clay-rich layers originating from the underlying Luvisol (MF Type 1.2, Fig. 7A and B). Three types of gravel deposits were identified: moderately sorted gravels with Luvisol aggregates (MF Type 3.1, Fig. 8A), moderately sorted gravels with poorly cemented sand coatings (MF Type 3.2, Fig. 8B) and moderately sorted sands and gravels with rounded carbonate clay aggregates (MF Type 3.3, Fig. 8C). As a result, this road presents a complex and stratified preparation layer compacted with plastic materials of different lithologies. The transit surface shows considerable reworking due to traffic (MF Type 2.2, Fig. 7D) that is only visible in thin section. The whole road deposit (preparation layers and traffic surface) is 22 cm thick.

**Road 2** This is limited to 3 microfacies units (preparation layer, traffic surface and reworked traffic surface) in a thin section (sample 9). It is only 5 cm thick and has been considerably reworked, especially on the margins of the road, where it is not appreciable with the naked eye. This seems to be an occasional repair of Road 1 by adding a thin preparation layer and a new traffic surface. This preparation layer is a different technical solution, since it is a new microfacies type (MF Type 3.5 with well-sorted gravels and no fine fraction, Fig. 8E) that gives way to a very porous, thin preparation layer (sample 9, mf unit 1). The traffic surface presents two microfacies. Whilst the first is well-preserved (MF Type 2.1, Fig. 7C), the second evidences considerable reworking towards the surface (MF Type 2.2, Fig. 7D).

**Road 3** This is only 10 cm thick and is a repair of Road 2 by raising the traffic surface (MF Type 2.1, Fig. 7C).

**Road 4** This road involves an important change in the use and repair dynamics identified in the previous roads, as it has a thick preparation layer of up to 38 cm (Figs. 6 and 9: stratigraphic unit 6). This layer reveals a new technical solution with the addition of moderately sorted fine sands with gravels (MF Type 3.4, Fig. 8D), which resulted in a porous sediment but more massive than previously described preparation layers. Above it, there is a traffic deposit showing an irregular surface (Fig. 6: stratigraphic unit 7).

**Road 5** This shows the same dynamic as Road 4, with a thick preparation layer (up to 31 cm) composed of several stratigraphic units visible in the field (Figs. 6 and 9: stratigraphic units 8–11). In thin section, they correspond to the same microfacies type (MF Type 3.5: well-sorted gravels without fine fraction, Fig. 8E). Overlying them, there is a well-preserved traffic surface with a very regular morphology (MF Type 2.1), perhaps indicating a short period of use.

**Road 6** This is truncated and only part of its preparation layer is documented (Figs. 6 and 9: stratigraphic unit 13). It shows the same technical solution as Road 5, with the addition of well-sorted gravels without fine fraction (MF Type 3.5, Fig. 8E).

### Lithological and elemental composition

The lithologies present in the coarse mineral fraction of the different microfacies are indicative of the source of the gravels used in the construction of each of the roads that make up the *Via Augusta* road sequence (Fig. 10). The main lithological difference is constituted by the Luvisol deposits in comparison to the road deposits. Luvisol deposits present a siliciclastic composition with large amounts of angular smooth quartz. However, the gravel deposits that make up the *Via Augusta* are composed of detrital clasts with rounded morphologies indicative of long transport and alluvial bed-load deposits.

Calcareous lithologies from different Tertiary biostratigraphic horizons and sedimentary depositional environments are dominant, constituting 50–70% of the coarse fraction of the deposits, although there are also siliciclastic gravels and, in minor proportions, igneous and metamorphic rocks. Whilst the proportions of these broad categories do not show significant differences amongst the deposits, there are a few details that are instead related to the source areas of these materials. Amongst the calcareous lithologies, bioclastic limestone stands out. Whilst they have a wide range of different biostratigraphic origins, those with nummulitid and quinqueloculina foraminifera are more frequent. Bioclastic limestone shows significant enrichments in samples 2–8 and 12 (Mf Unit 3) to 18 (Mf Unit 1) with minimum values of 38.46% and maximum values of 48.33%. According to the microfacies analysis, these samples correspond to Roads 1 and 5 of the road sequence (Fig. 11). In contrast, the rest of the samples show variable and lower values of between 0 and 16%. Dolomites are present in all samples with stable values (3.77–14.25%), with the exception of enrichments in samples 6 (Mf Unit 1), 8, 9 (Mf Unit 3), 14, 16 and 17 (Mf Unit 1), that show values of between 18.09 and 33.42%. These samples correspond to Roads 1, 2 and 5 (Fig. 11). Sparitic limestone is also generalised in the sequence, but in significantly smaller amounts (0.64 to 1.67% in Luvisol

**Table 2** Microfacies types identified in the stratigraphic sequence of the *Via Augusta*. These microfacies types are illustrated in Figs. 7 and 8. Microfacies analysis is shown in Figs. 9 and 12

Microfacies type	Subtypes	Description
<i>MF Type I, Luvisol</i>	1.1. Calcic Luvisol (Fig. 10: A)	This microfacies is a well-sorted clay with a silt-size mineral fraction. The coarse mineral fraction is composed of silt-size angular smooth quartz, silt-size angular smooth calcite and silt-size muscovite. There are also disorthic typic micritic nodules showing the same coarse mineral fraction of this soil in terms of mineralogy and grain size (silt-size quartz, calcite and muscovite), as well as decalcification features. Fine fraction is composed of brownish grey clay (both PPL and XPL). These components present a single-spaced porphyric c/f related distribution. Porosity is mainly composed of channels. Pedality is poorly developed, showing rare moderately to well-separated unaccommodated porous crumbs. This microfacies shows a massive microstructure and an undifferentiated b-fabric
	1.2. Reworked Calcic Luvisol (Fig. 10: B)	This microfacies is a moderately sorted clay with granular microstructure. Coarse mineral fraction is composed of silt-size angular smooth quartz, silt-size angular smooth calcite and silt-size muscovite. There are also disorthic typic micritic nodules that present the same coarse mineral fraction of this soil in terms of mineralogy and grain size (silt-size quartz, calcite and muscovite), as well as decalcification features. Fine fraction is composed of brownish grey clay (both PPL and XPL). These components show a single-spaced porphyric c/f related distribution. Porosity is mainly composed of compound packing voids. Pedality is well-developed, showing moderately to well-separated unaccommodated porous crumbs. This microfacies exhibits a granular microstructure and an undifferentiated b-fabric. As pedofeatures, a few sparitic calcitic pendants were identified

**Table 2** (continued)

Microfacies type	Subtypes	Description
<i>MF Type 2, traffic surfaces</i>	2.1. Traffic surfaces (Fig. 10: C)	<p>Coarse mineral fraction is composed of gravel-size clasts. Fine fraction is composed of a massive dark grey carbonate clay micromass (both PPL and XPL—described in detail in the text). These components show a double-spaced coarse enaulic <i>c/f</i> related distribution. Porosity is mainly composed of compound packing voids, while carbonate clay aggregates show its own porosity. Pedality is well-developed, presenting well-separated unaccommodated porous crumbs. This microfacies shows a massive to granular microstructure (which becomes massive at the top of the microfacies) and a crystallitic b-fabric. As pedofeatures, micritic pendants in gravel-size clasts are present. Physical disturbance and reworking due to trampling are very common, as shown by the features present related to traffic (see Sect. 4.2.3): fissures in clasts and subhorizontal fissure patterns within the micromass</p>
	2.2. Reworked traffic surfaces (Fig. 10: D)	<p>Coarse mineral fraction is composed of gravel-size clasts, sand-size angular smooth quartz, quartzite, slate and calcite with occasional sand-size rounded smooth basalt grains. Fine fraction is composed of sand to gravel-size subangular to subrounded carbonate clay aggregates (described in detail in the text). These components show a single-spaced equal enaulic <i>c/f</i> related distribution. Porosity is mainly composed of complex packing voids, while carbonate clay aggregates exhibit their own porosity. Pedality is well-developed, showing well-separated unaccommodated porous crumbs. This microfacies shows a granular microstructure and a crystallitic b-fabric. As pedofeatures, micritic pendants in gravel-sized clasts are present. Physical disturbance and reworking due to trampling are very common, as shown by the features present related to traffic (see Sect. 4.2.3): fissures in clasts and subhorizontal fissure patterns within the micromass</p>

**Table 2** (continued)

Microfacies type	Subtypes	Description
<i>MF Type 3, gravel deposits</i>	3.1. Gravel type 1: moderately sorted gravels with Luvisol aggregates (Fig. 11: A)	Coarse mineral fraction is composed of gravel-size clasts showing interstitial sand-size grains. This interstitial material is mainly composed of sand-size angular smooth quartz, quartzite, slate and calcite with occasional sand-size rounded smooth basalt grains. Sand-size rounded aggregates of well-sorted clay (from the Luvisol: microfacies Type 1) and sand-size disorthic micritic nodules and calcite aggregates are also common in the interstitial fraction. These components show a single- to double-spaced coarse monic <i>c/f</i> related distribution. Porosity is very high, showing compound packing voids. As pedofeatures, a few silt laminated cappings and micritic pendants in gravel-size clasts are present, sometimes linking grains and aggregates. There are also common sparitic calcite coatings around gravel-size grains
	3.2. Gravel type 2: moderately sorted gravels with poorly cemented sand coatings (Fig. 11: B)	Coarse mineral fraction is composed of gravel-size clasts with interstitial sand-size grains that most commonly correspond to poorly cemented sand coatings around gravels. Interstitial material is mainly composed of sand-size angular smooth quartz, quartzite, slate and calcite with occasional sand-size rounded smooth basalt grains. Porosity is very high, exhibiting simple packing voids. Regarding pedofeatures, there are very few sparitic calcite coatings and micritic pendants in gravel-size clasts, as well as poorly cemented sand coatings around grains
	3.3. Gravel type 3: moderately sorted sands and gravels with carbonate clay aggregates (Fig. 11: C)	Coarse mineral fraction is composed of gravel-size clasts with interstitial sand-size grains. Greyish carbonate clay aggregates are also frequent in this subtype. Interstitial material is mainly composed of sand-size angular smooth quartz, quartzite, slate and calcite with occasional sand-size rounded smooth basalt grains. This microfacies type shows a coarse monic <i>c-f</i> related distribution. Porosity is very high, exhibiting simple packing voids. Regarding pedofeatures, there are few sparitic calcite coatings and micritic pendants in gravel-size clasts
	3.4. Gravel type 4: moderately sorted fine sand with gravels (Fig. 11: D)	Fine sand-size clasts are mainly composed of fine sand (dominant) to gravel-size clasts. Fine sand-size clasts are mainly composed of sand-size angular smooth quartz, quartzite, slate and calcite with occasional sand-size rounded smooth basalt grains. This microfacies type shows a coarse monic <i>c-f</i> related distribution. Porosity is very high, exhibiting compound packing voids. As pedofeatures, a few silt laminated cappings and micritic pendants in gravel-sized clasts are present, sometimes linking grains
	3.5. Gravel type 5: well-sorted gravels without fine fraction (Fig. 11: E)	Coarse mineral fraction is composed of gravel-size clasts. This microfacies does not present interstitial sand-size grains or fine material. These components show a double-spaced coarse monic <i>c/f</i> related distribution. Porosity is very high, exhibiting simple packing voids. As pedofeatures, sparitic and micritic pendants in gravel-sized clasts are present, sometimes linking grains as cappings



deposits and 1.28 to 12.56 in gravel deposits) with the notable exception of the microfacies units on the traffic surfaces of Roads 1 and 5, which show higher values (sample 9 Mf Unit 1 with 32.62% and sample 18 Mf Unit 2 with 51.16%, respectively) and the upper part of the traffic surface corresponding to Road 3 (sample 11). Micritic limestone is also omnipresent in the gravel deposits and shows a significant increase in samples 9–14 with values of up to 67.81% (Roads 2–4 and the lower part of Road 5), whilst in the rest of the samples, it is lower than 10% (Roads 1 and 5). Other sedimentary rocks such as sandstone are residual and only present in Samples 10 and 13 (Roads 3 and 5).

Siliciclastic gravels are composed of quartz and flint. Quartz is present in all the samples and shows significant differences throughout the sequence. Coarse fraction in Luvisol deposits is mainly composed of silt-size angular smooth quartz grains (samples 1–3 with 96.64–98.33%), whilst the gravel deposits of the *Via Augusta* show two different quartz grain sizes: interstitial smooth angular sand-size grains, on the one hand, and rounded gravel-size grains, on the other (Fig. 11). Whilst quartz has a homogeneous distribution throughout the different roads (10–25%) with some exceptions (sample 15 at 54.51%), Road 5 stands out as it has lower values (less than 10%). Flint, however, is residual in this lithological assemblage, being especially present in Roads 4 and 5 (samples 10–18) with values lower than 5%.

Igneous and metamorphic rocks such as basalt, granite, slate and quartzite are present in the sequence with residual values (Fig. 11). Whilst quartzite and basalt distribution is homogeneous throughout the sequence (normally less than 10% and 5%, respectively), slate is more abundant in Roads 2–4 (samples 6–12) and granite is only present in Road 5 (sample 18 mf unit 1).

These lithologies and their proportions in the gravel deposits of the *Via Augusta* can be assigned to a source area: the lower terrace and alluvial deposits of the River Guadalquivir (Fig. 3B: 5 and 7). According to previous mineralogical and lithological studies undertaken in the area (Lorite-Herrera et al. 2008; Jimenez-Espinosa et al. 2016), these units mainly consist of dolomite, calcite, quartz, clay minerals and feldspar, with a large amount of carbonate lithologies representing more than 40% of the lithological assemblage. This predominance of the carbonated lithologies is shown through  $\mu$ -XRF. The analysis reveals a majority presence of carbonated materials and minor amounts of siliciclastic and metamorphic materials (Fig. 12). Whilst the basal levels are calcitic-rich and show micritic, microsparitic and fossiliferous limestones, dolomite increases in the upper levels, revealing a fine-grained matrix poor in phyllosilicates. Calcitic-rich deposits of the basal levels come from the Neogene sediments that comprise the substrate of the Guadalquivir basin and the Mesozoic Subbetic rocks of the Sierra Mágina area (Fig. 3A). Dolomitic-rich deposits

originate in alluvial sediments from the Mesozoic Prebetic rocks of the Sierra de Cazorla and the blocks containing Triassic sediments included in the Olistostromic unit of the Guadalquivir basin (Fig. 3A). The basal deposits also contain Palaeozoic metamorphic and igneous materials such as quartzite, slate, granite and basalt originating from soil formations in the Sierra Morena (Fig. 3A) washed down by the River Guadalimar that flows into the Guadalquivir a few kilometres further up the basin.

The lithological assemblage identified in this section of the *Via Augusta* where it passes through the *Ianus Augustus* has rocks from both the basal (bioclastic limestone, micritic and microsparitic limestone, Palaeozoic materials) and upper levels (dolomite) of the lower terrace of the River Guadalquivir, as well as from recent alluvial deposits. However, there are slight differences in the proportions of these materials throughout the sequence. Roads 1 (Fig. 11: sample 2 mf unit 3 to sample 8) and 5 (Fig. 11: sample 12 mf unit 3 to sample 18) exhibit an increase in bioclastic limestone, dolomite, sparitic limestone and, in the case of Road 5, also quartz and flint, with these lithologies common in both the basal and upper deposits of the lower terrace (Fig. 11). However, Roads 2, 3 and 4 (Fig. 11: samples 9 to 12 mf unit 2) show higher quantities of micritic limestone and igneous and metamorphic rocks, typically from basal levels (Fig. 11). Even though the source area was the same for the repairs carried out during the active life of the road (the lower terrace of the River Guadalquivir and recent alluvial deposits), perhaps different horizons were exploited for Roads 2–4 (basal levels) and Roads 1 and 5 (a mix of basal and upper levels). Although, further detailed mineralogical analysis of the source area and the gravel deposits of the road considering larger samples will be needed to confirm this interpretation, since these data come from a single sondage.

Regarding traffic surfaces, the fine mineral fraction is composed of massive dark grey carbonate clay with muscovites, microlayering, a massive microstructure and a crystallitic b-fabric (Figs. 7C and 13G). This lithology is not present in the layout of the *Via Augusta*, which at this point is set on a Luvisol of brownish grey clay (both PPL and XPL). The nearest source for such materials is the Upper Miocene Porcuna Unit of yellowish grey marls (Fig. 3: 1) 2.5 km south to the studied section of the *Via Augusta*.

### Sedimentary structures and features

These deposits show some characteristics typical of the effects of trampling in coarse components (Rentzel et al. 2017). They exhibit preferred orientations parallel to the surface and a strong imbrication of coarse components (Figs. 7C). Clasts displaying microfractures are common. Whilst these fissures could be natural in some clasts (Fig. 13D), others reflect in situ breaking by shearing and

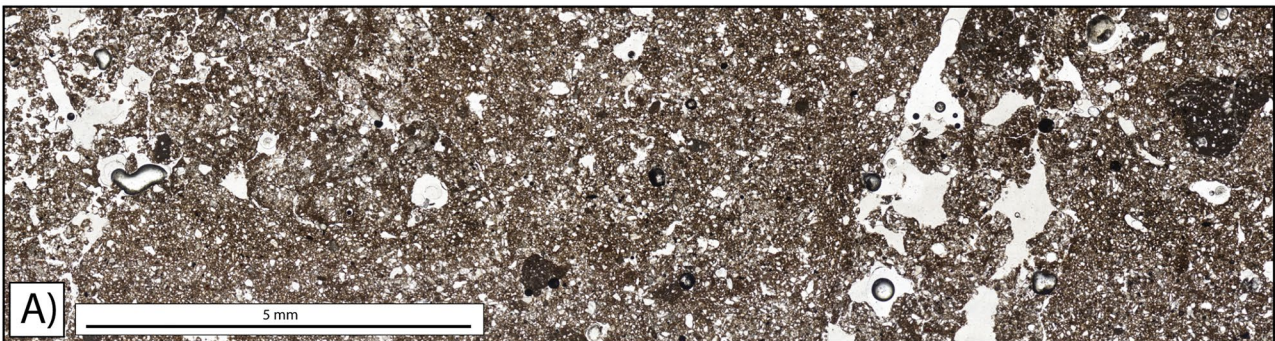
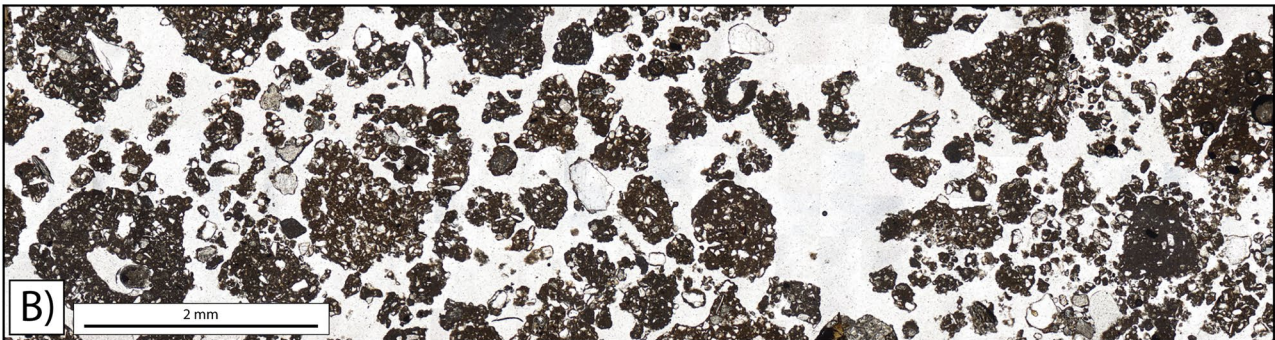
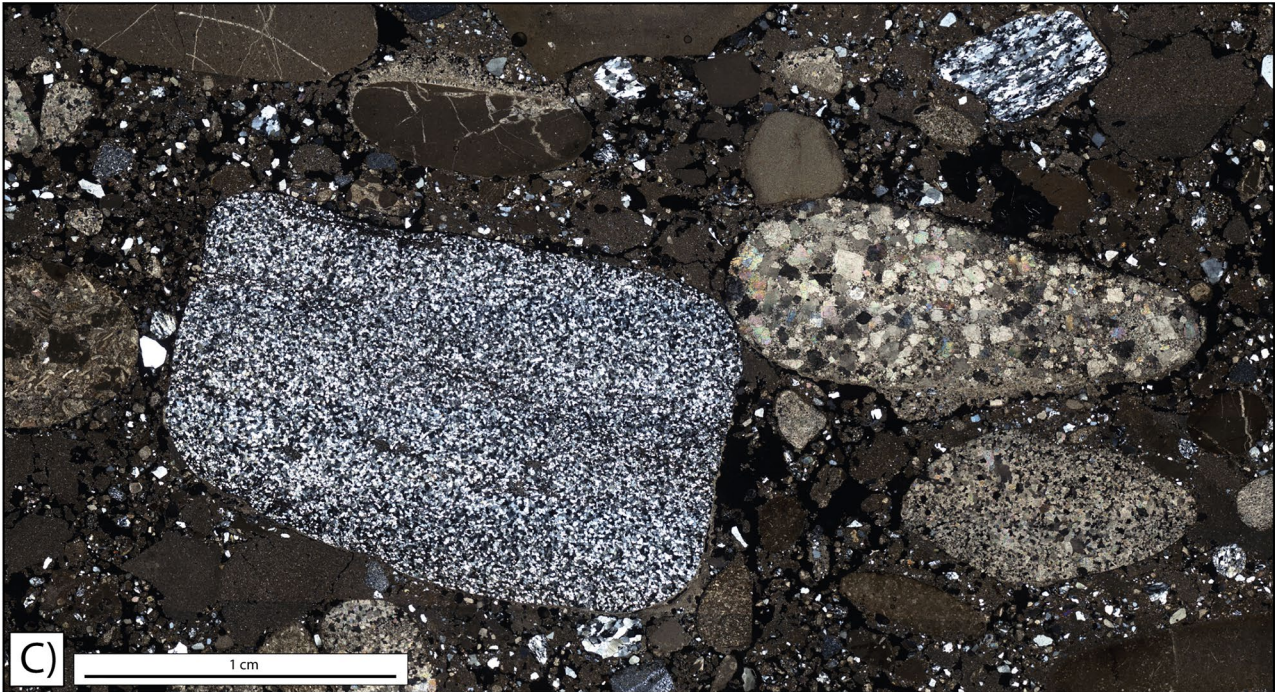
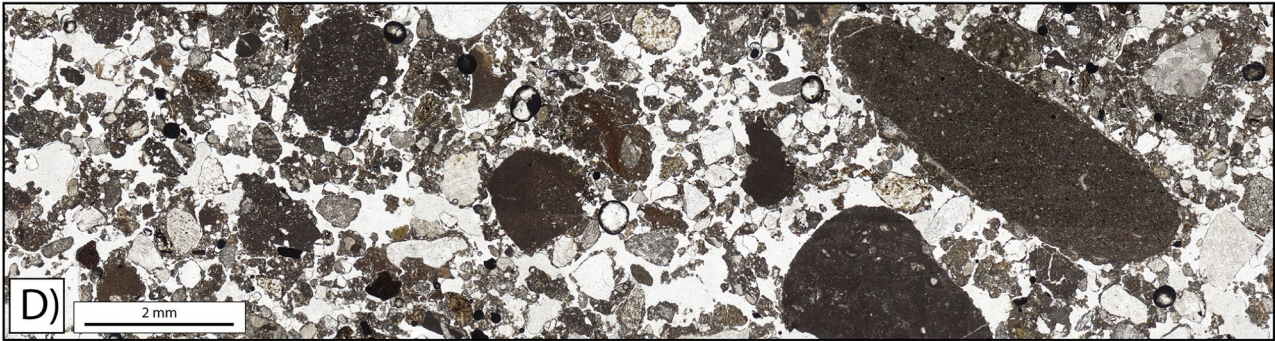


**Fig. 7** Microfacies analysis (I). **A** Microfacies type 1.1. Calcic Luvisol; **B** Microfacies type 1.2. Reworked Calcic Luvisol; **C** Microfacies type 2.1. Traffic surfaces, showing a clay carbonate micromass; **D** Microfacies type 2.2. Reworked traffic surfaces, showing a clay carbonate micromass

later infilling of the fissures with the surrounding clay carbonate (Fig. 13E). These features are related to technical solutions applied during construction, by trampling and applying considerable pressure to the deposits to the point of breaking some of the clasts. Some clasts also show calcitic pendants (Fig. 13C) and features that, rather than cappings, would, in our opinion, be upside down calcitic pendants (Fig. 13B). In this respect, these pendants, along with poorly cemented sand coatings around grains, would be relicts of post-depositional processes in their original sedimentation environment, the lower fluvial terrace of the River Guadalquivir. In other cases, silt coatings indicate water infiltration depositing silt and clay particles (Fig. 13A).

The transit surfaces show structural modifications due to the effect of traffic. Carbonate clay micromass exhibits massive to granular microstructure, bedding and subhorizontal fissure patterns related to strong compaction during the construction process and later disaggregation due to vehicle traffic (Rentzel et al. 2017) (Fig. 13F and G). Similar fissures were reported by Charbonnier and Cammas (2018) in Roman roads in France.

### Textural parameters

Percentages of porosity, grains—sand and gravel fractions—and micromass, understood as the fine material of the deposits, composed of clay, fine silt and coarse silt (Stoops 2003, p. 93; Stoops and Mees 2018, pp. 74–75), were analysed through image analysis and segmentation. There are significant differences amongst these deposits depending on their nature. In this respect, the traffic surfaces (Fig. 14B: samples 10–12, 15, 23 and 24) stand out due to the low variability of the porosity percentage, which is particularly regular in the traffic surfaces 2 (14.08%), 3 (16.29%) and 4 (17.74%). Traffic surfaces 1 (25.94%) and 5 show different values (7.77 and 26.39%) due to the considerable reworking of traffic surface 1 and the use of larger clasts on traffic surface 5, which produced a more developed simple packing void porosity. This tendency is also highlighted for the clast percentages that again are very regular on the traffic surfaces and show values between 50.11 and 59.97% of the deposit. Finally, this tendency is also visible in the percentage of micromass, with values of between 28.57 and 34.37%. In contrast, gravel microfacies types (Fig. 14B: samples 2, 4, 5, 7–9, 13, 14, 16–22 and 25), interpreted as preparation layers, show a more variable porosity throughout the deposit, ranging from 7.04 to 44.37%. These variances do

not show any correspondence with the five gravel types identified in micromorphology. The clast percentages, however, are more homogeneous and show values of between 54.46 and 74.85%, with quite a few values above 70% in this sequence. The same situation is identified in the micromass percentages, which range from 0 to 19.36%. Samples 3 and 6 (Fig. 14B), characterised as reworked Luvisol deposits, are interpreted as sandy clay preparation layers with more micromass and less coarse fraction. These two samples show similar porosity values (37.38–34.22%), clasts (27.79–30.76%) and micromass (34.83–35.02%). Finally, the local Luvisol below the *Via Augusta* (Fig. 14B: sample 1) shows very different values compared to the preparation layers and traffic surfaces: the micromass percentage is significantly higher (58.70%), whilst clasts (18.16%) and porosity (23.03%) show lower values.

In the textural parameters of the coarse fraction, there are significant differences amongst the microfacies types identified in micromorphology (Figs. 7, 8 and 15). Grain size is explored in the parameters of area (measured in pixel counting) and equivalent circular diameter. Area histograms reveal skewed left patterns in all the microfacies types (Fig. 15). Whilst the Luvisol shows a predominance of well-sorted fine quartz sands (predominance of the categories 15.94 and 27.81 in area), the Luvisol deposit between the soil and the preparation surface of the first traffic surface shows a greater variability in grain sizes, which are larger than the typical fine quartz sands of the Luvisol. The road deposits are, on the one hand, mostly homogeneous (with the predominant values ranging between 140 and 830), although Gravel Type 1 shows a heterogeneous mix of grain sizes compared to the other 4 gravel types. On the other hand, the gravel sizes in the road deposits are quite similar for Gravel Types 2–4 (140–415 pixels), whilst they are significantly larger in Gravel Types 1 (upwards of 1255 pixels) and 5 (upwards of 430 pixels). Finally, the grain size in traffic surface deposits is larger than in most of the other gravel types and better sorted (predominance of the categories 806.31 and 901.80 in area). With respect to the equivalent circular diameter (Fig. 15), whilst the histograms of all microfacies types show skewed left patterns, there are differences amongst them. Some types, such as Gravel Types 2–5, the reworked Luvisol and especially the Luvisol, show good classification and sorting. In all those cases, the values are distributed in the lowest classes of the histogram. In contrast, the rest of the microfacies types show heterogeneous distributions and a major presence of larger grain sizes. This is the case of Gravel Type 1 and the traffic surfaces, which combine fine sands with different gravel sizes.

Orientation histograms (Fig. 15) exhibit multimodal patterns in all microfacies types, except for Gravel Type 5. In road deposits, Gravel Types 1–4 show a predominance of vertical (84.38°) and horizontal (174.38°) orientation of

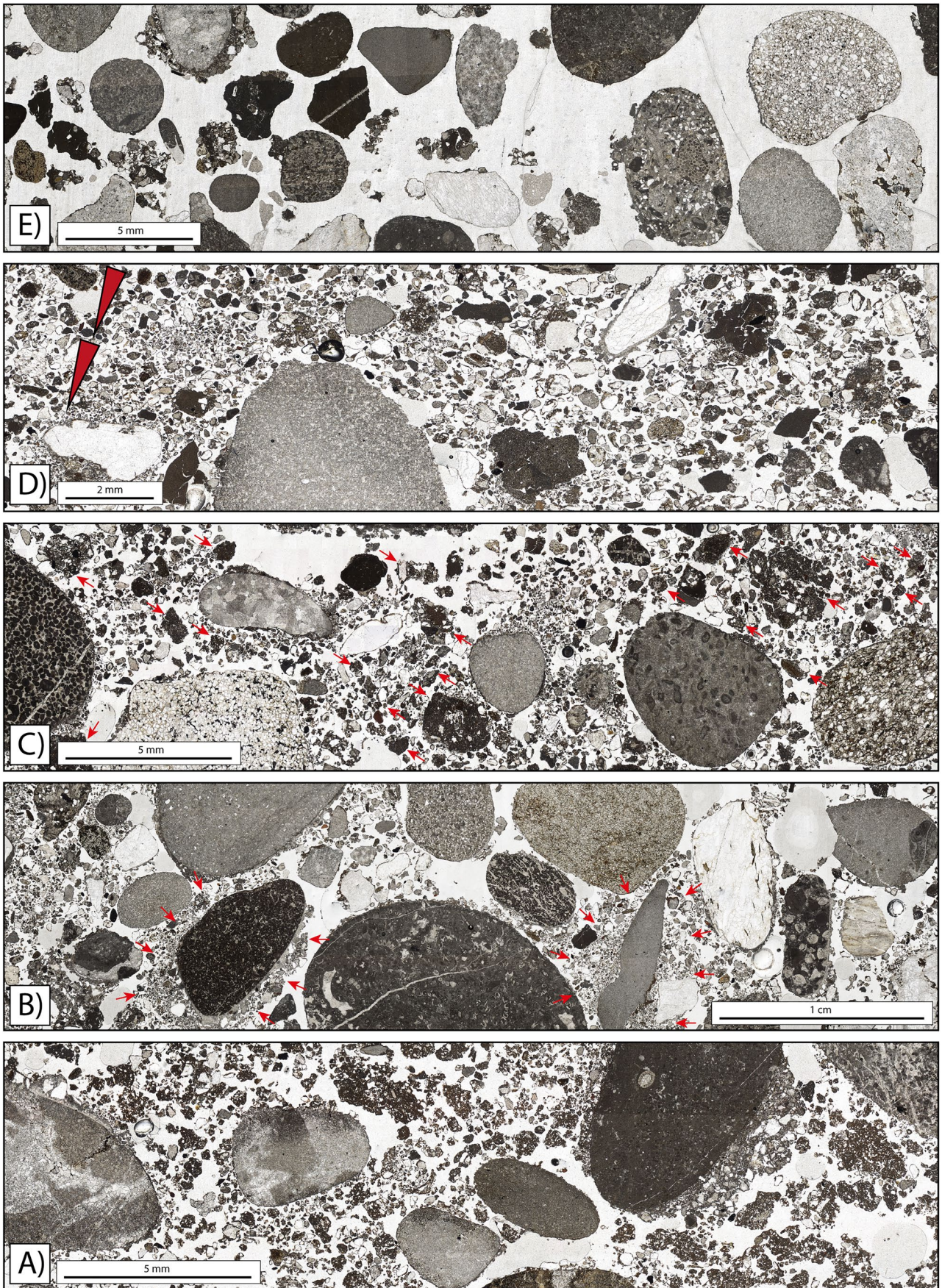


**Fig. 8** Microfacies analysis (II). **A** Microfacies type 3.1. Gravel type 1: moderately sorted gravels with Luvisol aggregates; **B** Microfacies type 3.2. Gravel type 2: moderately sorted gravels with poorly cemented sand coatings (red arrows indicate two poorly cemented sand coatings); **C** Microfacies type 3.3. Gravel type 3: moderately sorted sands and gravels with carbonate clay aggregates (red arrows indicate some of the abundant aggregates); **D** Microfacies type 3.4. Gravel type 4: moderately sorted fine sand with gravels (red triangles indicate reverse grading); **E** Microfacies type 3.5. Gravel type 5: well-sorted gravels without fine fraction

gravels and sands. Gravel Type 5 stands out for a symmetrical pattern distribution of the histogram, which is indicative of a greater diversity of orientations in the coarse fraction. It must also be noted that this coarse fraction in Gravel Type 5 is very rounded. In contrast, the traffic surfaces show a significant horizontal orientation of gravels ( $174.38^\circ$ ), similar to the reworked Luvisol deposits. In both cases, this is indicative of trampling and surface compaction during construction. The Luvisol, on the other hand, has a greater diversity of orientations. However, it must be noted that the coarse material in this deposit is composed of angular smooth fine quartz sands, making it difficult to characterise the orientation.

Compactness and elongation (Fig. 15) refer, in this case, to the roundness of the sands and gravels (in both cases expressed in values 0–1, with 1 being a sphere). In terms of compactness, the histograms present different patterns according to the microfacies types. The traffic surfaces show a skewed right pattern with a tendency to roundness. The gravel deposit compactness histograms are more variable. Whilst Gravel Types 1 and 3 show a skewed right pattern and a tendency to roundness, Gravel Types 2, 4 and 5 present a skewed left pattern, indicating a majority presence of other grain morphologies. Finally, the elongation histograms show symmetric unimodal patterns, except for Gravel Type 1, which presents a bimodal pattern. Whilst Gravel Type 5 and reworked Luvisol deposits show a totally symmetric unimodal pattern, indicating a heterogeneous mix of grain morphologies, the rest of the microfacies types show a significant frequency of 0.64–0.78 and, only in the cases of Gravel Type 1 and the traffic surfaces, a second significant frequency of 0.98. For the first frequency, this indicates a majority presence of elliptical grains and, for the second, the occurrence of rounded grains.

## Discussion

A microstratigraphic analysis of the *Via Augusta* where it passes through the *Ianus Augustus* has made it possible to characterise the sequence, materials and construction techniques of the main Roman road in *Hispania*. It has also allowed the identification and analysis of this monumental

complex, an interprovincial border between *Hispania Baetica* and *Tarraconensis*. The results obtained show, in the first place, the need to reopen the debate into Roman roads. As we mentioned in the “Introduction” section of this study, an equivocal translation of Bergier’s work on Roman roads (1622) has led to an erroneous premise regarding these roads: a long tradition of studies that refer to a hypothetical construction scheme that is static and rigid and differs substantially from the archaeological reality, as we have seen throughout this paper and in other studies (Charbonnier and Cammas 2015, 2018; Garilli et al. 2017). Interdisciplinary analysis of the *Via Augusta* has confirmed that its builders possessed considerable technical expertise. Roman roads were as variable as their number and extension: they were adapted and subjected to the needs of wheeled vehicles and traffic, the geographical conditions of the environment in which they were located and the raw material resources available in their vicinity. This analysis corroborates and restores the validity of Bergier’s original words aimed at inspiring further research, which should focus on “the materials found in different layers [of the roads], their order, assigning each one a name and making them distinguishable” (free translation of Bergier 1622, p. 142).

At the microscale, the different geoarchaeological analyses undertaken were helpful in unravelling the road sequence. In this respect, we identified the superposition of 6 different roads through microfacies analysis (Figs. 7–9 and 12). This denotes a long biography of use and an interest in keeping the road in good condition for traffic. Two different repair dynamics were identified. Whilst Roads 2 and 3 consisted of repairing the traffic surface by reflooring it with thin preparation layers, Roads 4–6 present thick constructive fillings involving a large amount of raw materials and labour. Roads 4–6, therefore, can be understood as major repair works, perhaps of considerable scope, along the length of the *Via Augusta*. The materials used and their sources were determined through a detailed lithological study and by exploring the elemental composition of the deposits with  $\mu$ -XRF (Figs. 10–12). Our study revealed a careful selection of the materials used according to their functions. Those materials—carbonate clay for traffic surfaces and fluvial gravels for construction infills—were sourced locally, less than 2.5 km from the studied road section (Fig. 3). This careful selection of the materials was explored in more detail by studying the textural parameters of the deposits through image analysis and segmentation which, after investigating the different variables (Table 1), provided a fingerprint of these deposits (Figs. 14–15). Textural parameters, along with micromorphology, were indicative of the techniques and technical solutions adopted during the construction of the road. The porosity, fine material and clast percentages in the deposits presented similar values for traffic surfaces, which denote a specific solution or mixing of materials

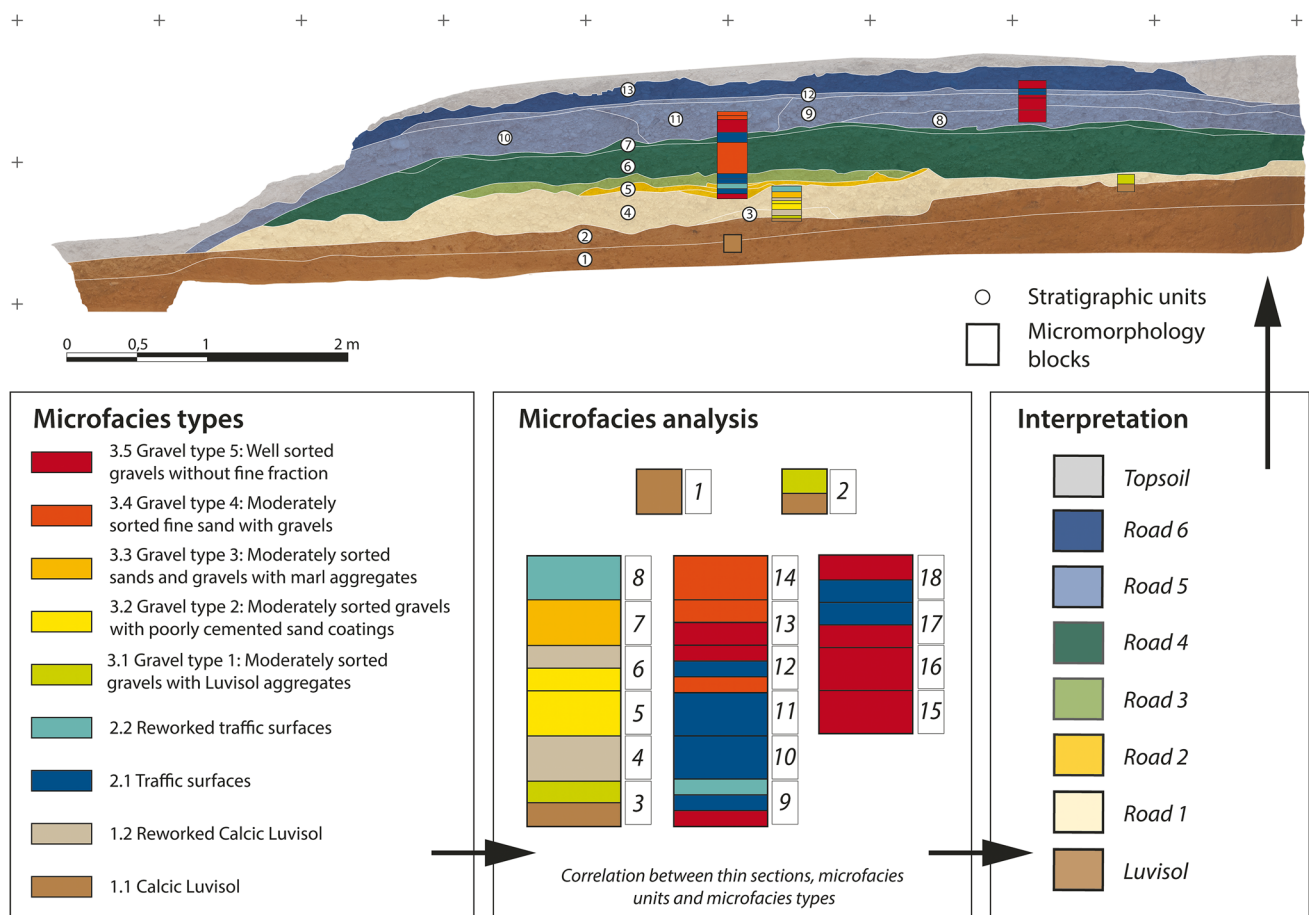


**Fig. 9** Microfacies analysis of the *Via Augusta* deposits

during construction. The fact that these values were similar amongst the different roads is indicating that this technical knowledge was maintained across the entire active life of the road. The percentages for the gravel construction infills were more variable, which fits in with the 5 microfacies types identified in the micromorphology (Figs. 7–8, Table 2). These microfacies types can be understood as five different construction techniques. The techniques were explored more in detail by studying certain parameters of the coarse mineral fraction in the studied deposits (Fig. 15). Grain size, expressed in area and equivalent circular diameter, showed the homogeneous sizes of the clasts used in preparation layers, both individually and, in general terms, amongst the six roads identified. Despite this, Roads 1 and 5 had slightly bigger clasts.

The traffic surfaces and gravel deposits identified on the *Via Augusta* reveal specific sedimentary structures and features related to the technical solutions applied to the road building, such as dumping, compaction, trampling and shearing. In this respect, sedimentary structures and features visible in thin section are indicative of the way in which the road was built. As shown in the microfacies analysis, these deposits of imbricated, well-rounded, ellipsoidal and

discoidal fluvial gravels present local differences in and amongst them regarding sedimentary structures and bedding. Whilst most of the layers have a heterogeneous distribution of the coarse fraction (Fig. 6), all locally show reverse grading, which is more evident in thin sections (Fig. 13H). On the one hand, dumping may cause grading within the deposits (Karkanas and Goldberg 2019, p. 3), on the other, this sedimentary structure is very similar to dry grain flows (Bertran and Teixier 1999; Nemeč and Steel 1984). The typical bouncing of grains against each other during the downslope movement of large masses of rock leads to a downward movement of finer clasts at the base of the flow, whilst the coarse clasts become concentrated on the surface (Karkanas and Goldberg 2019, p. 38). Dumping of gravel materials from a certain height during the road construction thanks to the use of a wooden structure would not have been very different, from a sedimentary point of view, to a dry grain flow. Thus, a phenomenon of kinematic sieving could explain the recurrent reverse grading observed in thin section. Also, clast orientation offered information about how they were compacted during construction. Due to the pressure, some clasts show in situ fissures that are sometimes filled

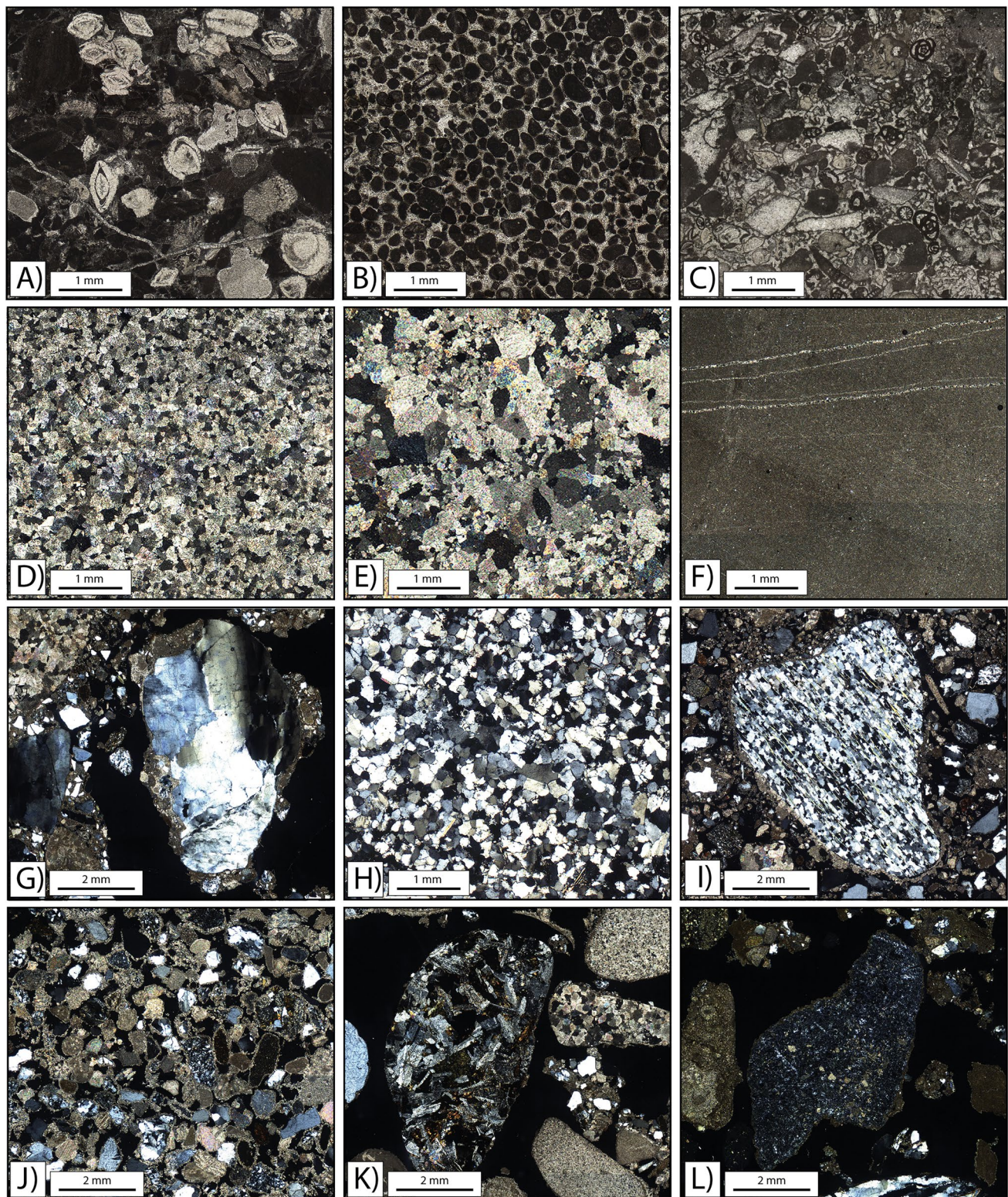


**Fig. 10** Most common lithologies in gravel deposits: **A–C** bioclastic limestone; **D** dolomite; **E** sparitic limestone; **F** micritic limestone with sparitic and microsparitic veins; **G** quartz; **H** quartzite; **I** slate; **J** poorly cemented sandstone; **K** basalt and **L** flint





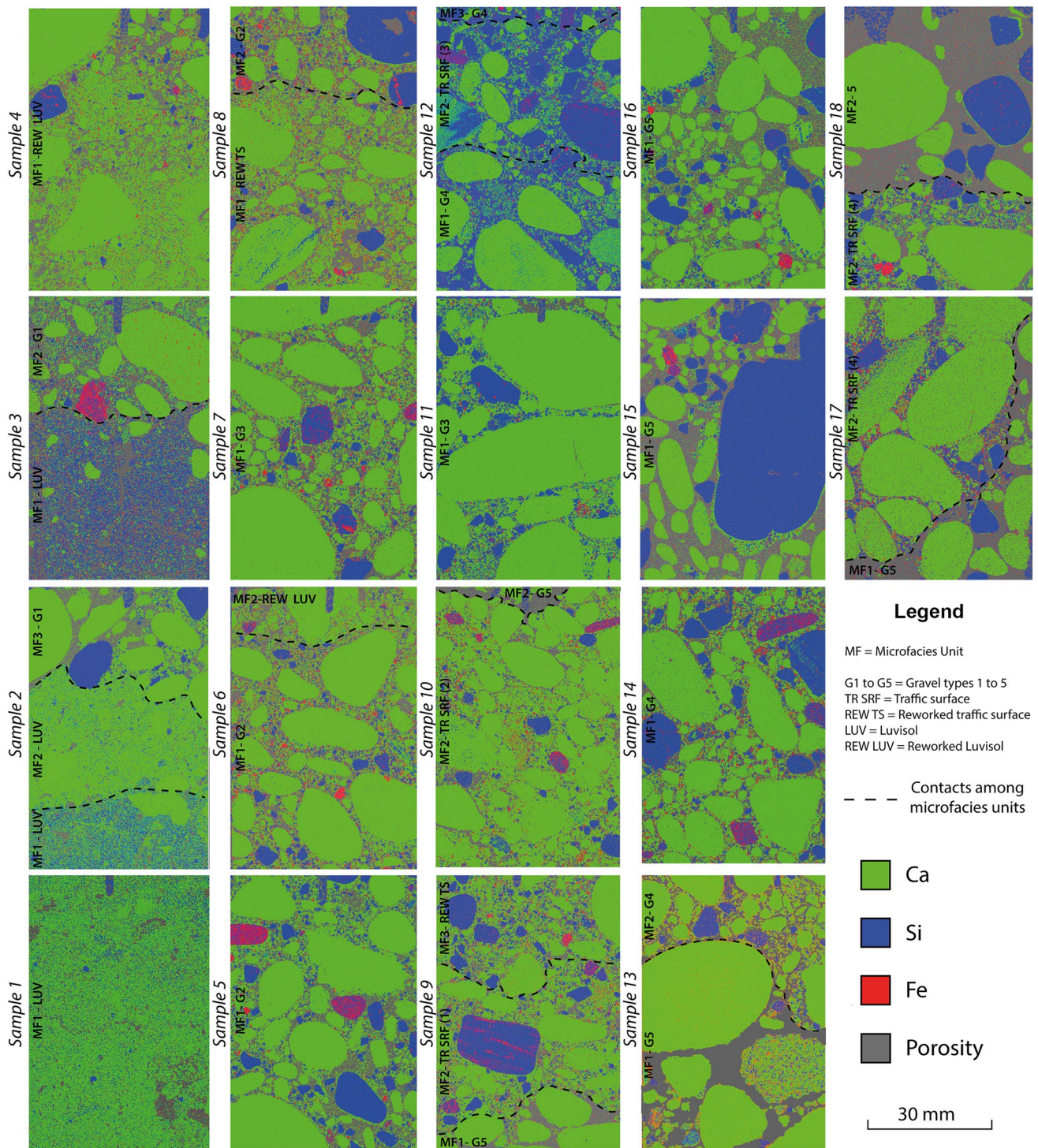


**Fig. 12** Elemental distribution of Ca, Si and Fe through  $\mu$ -XRF in relation to samples and microfacies analysis

with fine material. In order to cause these features, considerable pressure would have been applied, perhaps using a machine mentioned in literary and iconographic sources such as the *cylindrum*. This machine consisted of an animal-drawn stone roller, which employed a heavy stone column that rolled over

the gravel deposits, compacting them (González Tascón and Velázquez Soriano 2004, p. 208), and could exert the pressure enough to in situ fissure and broke the gravels and create the parallel sedimentary structure and horizontal orientation of the gravels along the many kilometres in the *Via Augusta* layout.

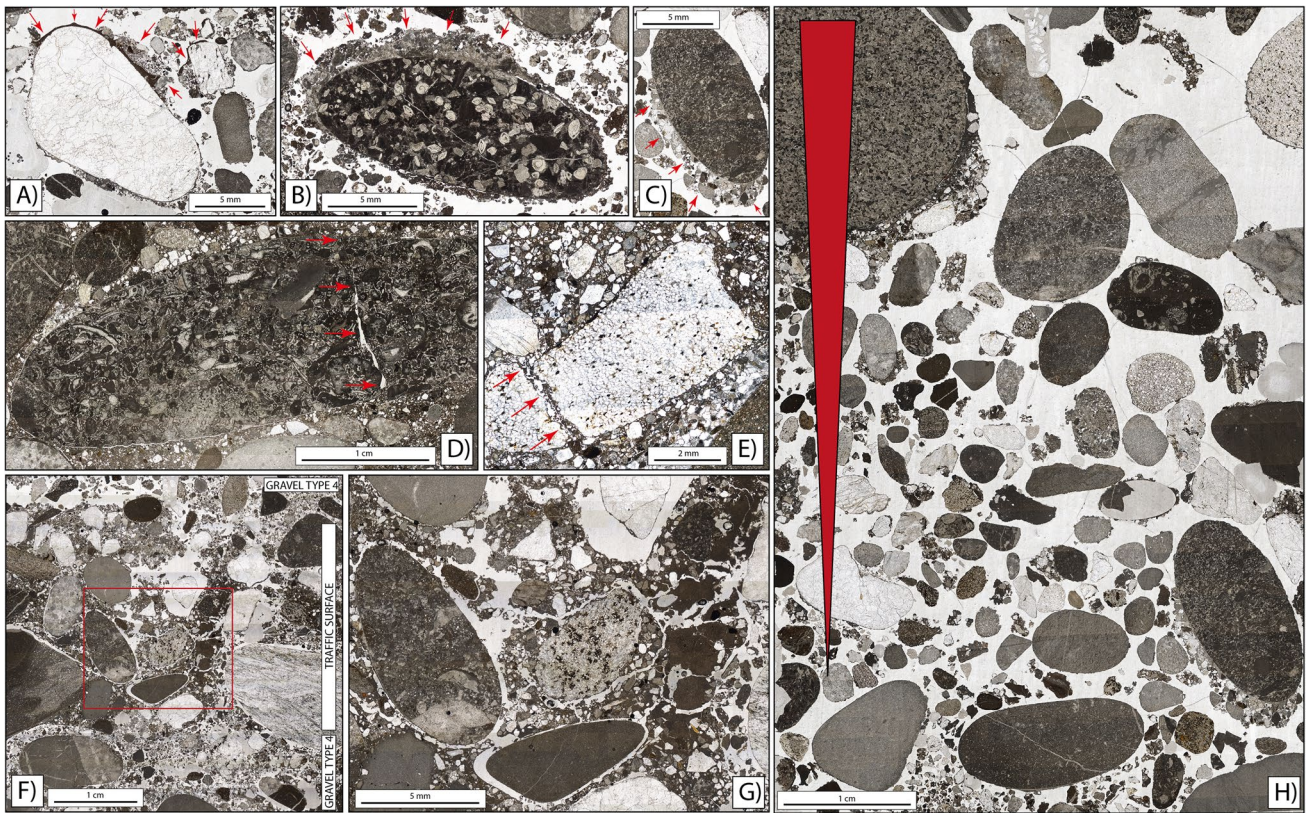


**Fig. 13** Features present in gravel and traffic deposits. **A** Silt coatings showing water infiltration depositing silt and clay particles; **B** upside-down calcitic pendant as a postdepositional relict of the original sedimentation environment of the clast; **C** calcitic pendant (post-depositional relict); **D** fissure of a clast, indicative of trampling; **E** fis-

sure of a clast filled with carbonate clay, indicative of trampling; **F** traffic surface in between gravel deposits. The red rectangle indicates Fig. 13G. **G** Subhorizontal fissure patterns and planar voids around grains resulting from traffic; **H** high-resolution scan of sample 16 showing reverse grading due to kinematic sieving

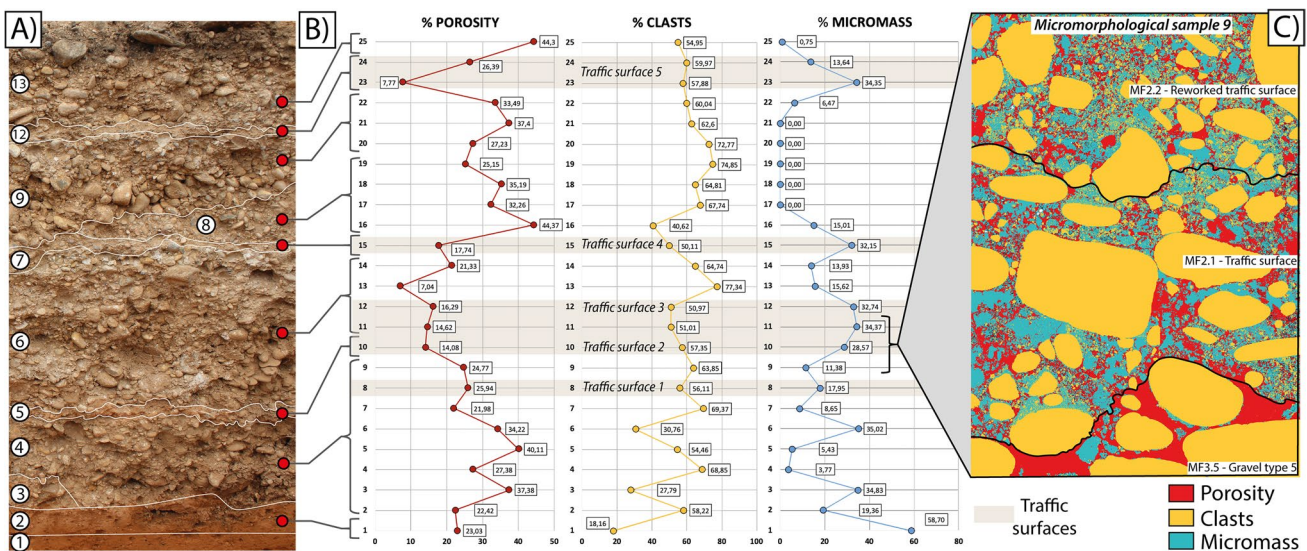


**Fig. 14** Textural parameters of the deposits on the *Via Augusta* (I). **A** Stratigraphic sequence showing the location in depth of the microfacies analysed (red points); **B** percentages of porosity, clasts and micromass of the whole sequence, indicating the traffic surfaces identified.

**C** Example of image analysis and segmentation of porosity, clasts and micromass of one thin section (analysed with JMicroVision 1.3.3). This thin section shows a preparation surface (MF1), a traffic surface (MF2) and a reworked traffic surface (MF3)

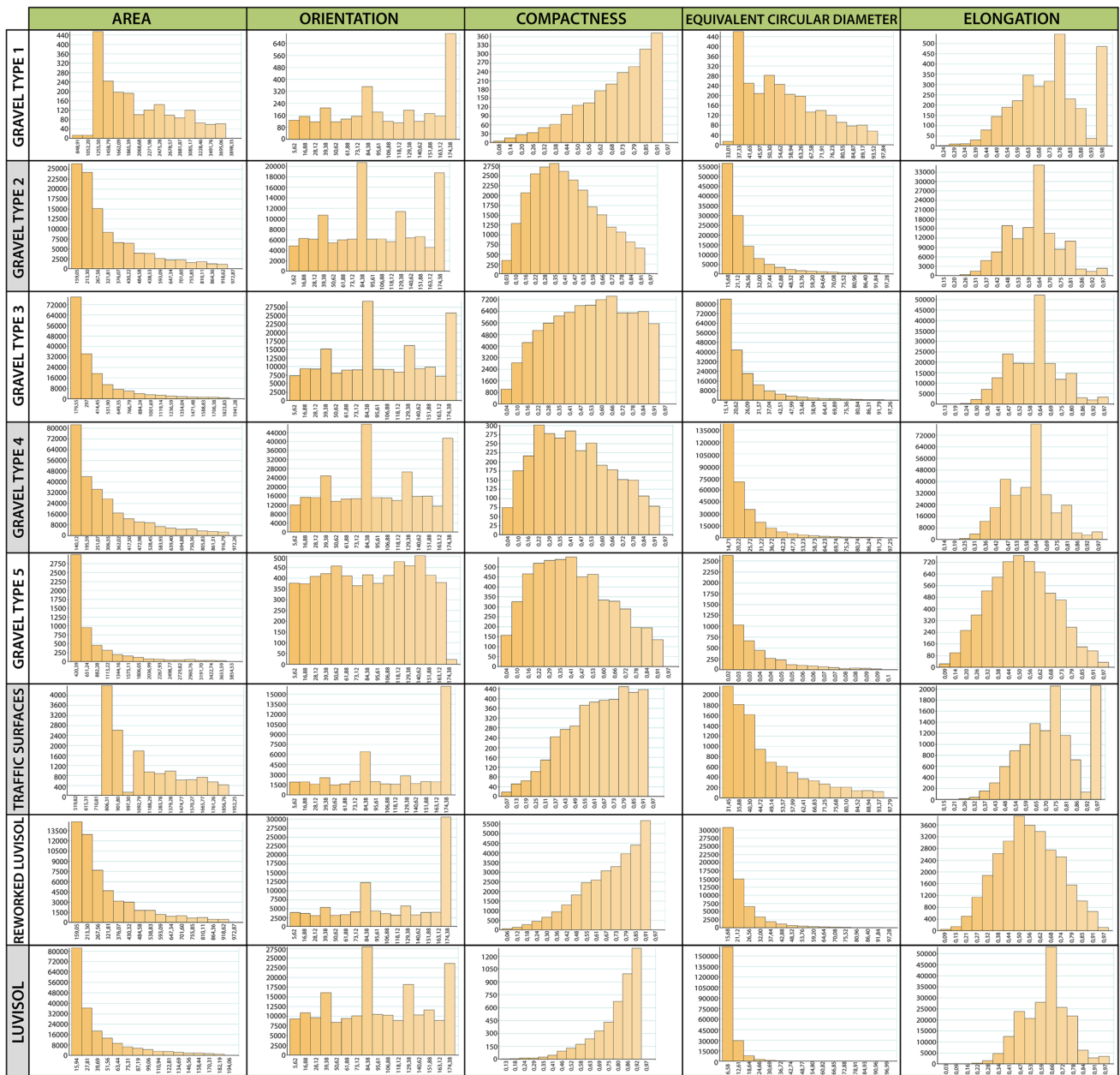


**Fig. 15** Textural parameters of the *Via Augusta* coarse mineral fraction deposits (II). Histograms of the area, orientation, compactness, equivalent circular diameter and elongation of the coarse mineral fraction of the different microfacies type deposits

The different repairs to the road observed through microfacies analysis are significant, as several repair projects carried out on the *Via Augusta* are documented on milestones from *Hispania Baetica* (Roldán Hervás 1975; Sillières 1981, 1990, 1994; Corzo Sánchez and Toscano San Gil 1992; Melchor Gil 1994, 2008; Schmidt 2013, 2018; Baltrusch et al. 2016; España-Chamorro 2017; España Chamorro 2019). At present, some fifteen epigraphs are preserved, amongst them milestones and inscriptions documenting bridge repairs that refer to the *Ianus* (Sillières 1994; España-Chamorro 2017; España Chamorro 2019). At least a third

of them retain the numeral, i.e. the distance from the point where the milestone was located to the *Ianus Augustus*. The references to this *caput viae* vary depending on the period to which each inscription belongs: *A Baete et Iano Augusto ad Oceanum* (CIL II, 4701, 4703, 4704, 4723, 4707, 4708, 4709, 4711, 4716, 4717 and 6208) in the period between Augustus and Caligula; *Ab Iano Augusto qui est ad Baetem usque ad Oceanum* (CIL II, 4715 and 4712) in the time of Tiberius; *Viam Augustam ad Iano ad Oceanum* (CIL II, 4718) between the Claudian and Domitian periods and finally, more explicitly, *Ab Arcu unde incipit Baetica Viam*

*Augustam militarem* (CIL II, 4721) in the time of Domitian. The last of these translates as “from the arch where *Baetica* starts”. These inscriptions commemorate the construction of the Imperial road by Augustus (CIL II, 4701, 4711, 4707, 4708, 4709 and 4704) and the commitment of his successors in maintaining the road and enriching it with more milestones (CIL II, 4715, 4716, 4712, 4717 and 6208). From Claudius on, and especially under Domitian, most of the epigraphs explicitly and repeatedly mention repair work along the road (“*viam Augustam militarem vetusta corruptam restituit*”). However, we do not know their scope, being it impossible to determine whether they were specific or general repairs along its layout within the provincial territory (CIL II, 4718, 4697, 4703, 4721, 4722, 4723 and CIL II/5, p. 65 no. 10).

It is impossible to date the different roads of the sequence identified or to evaluate their chronology and duration of use, due to the lack of finds in the construction deposits. Nevertheless, we believe that the repairs identified in the regional epigraphy can be associated in relative terms with those documented in our excavation. In this respect, the different repairs identified show that the road was heavily used and was therefore a very important communication hub within the road network. Although all the scholars who have studied the Roman roads in this area agree that the *Via Augusta* ran through the *Ianus Augustus* (Sillières 1981, 1990, 1994; Corzo Sánchez and Toscano San Gil 1992; Schmidt 2013, 2018; Baltrusch et al. 2016; España-Chamorro 2017; España Chamorro 2019), there is some debate within regional archaeology on the layout of the *Via Augusta* between *Corduba* and *Castulo* (Figs. 1 and 2). J.M. Roldán Hervás, C. Caballero Casado and P. Sillières suggest that it ran parallel to the River Guadalquivir, linking *Corduba* to *Castulo* via *Ad Decumo*, *Sacili*, *Ad Lucos*, *Epora*, *Vcia* and *Ad Noulas* (Fig. 2A) (Roldán Hervás 1975; Sillières 1976, 1990; Roldán Hervás and Caballero Casado 2014). Thus, it would be possible to identify the *Via Augusta* as the “Camino de los Romanos” road (Sillières 1976, p. 30). Sillières, following the hypothesis put forward by Holland (1961), described the *Ianus* as an arch across the river at the end of this road (Sillières 1981, p. 258) (Fig. 2B). He also hypothesised that there would have been a monumental building devoted to the Imperial cult to Augustus whilst he was still alive, making it one of the earliest examples of his worship (Sillières, 2003: 278). However, based on the route referred to in the Antonine Itinerary as *Iter a Corduba Castulone*, M.G. Schmidt proposes that this would have been an alternative route and not the main one. Moreover, Schmidt suggests an alternative location for the *Ianus* itself, on the River Guadalbullón (Schmidt 2018) (Fig. 2B). A. Ventura Villanueva agrees with this having studied a milestone reused in Bujalance castle that mentions the *Via Augusta* and the *Ianus* (Ventura Villanueva 2013). Both scholars believe that the main route of the *Via Augusta* would have connected

*Corduba* and *Castulo* via an interior route through *Calpurniana*, *Obulco*, and *Vrgavo* (Fig. 1). This opinion of the northern road following the river as the *Alio itinere* or alternative road and the southern and inner one as the main route of the *Via Augusta* has been followed by Melchor (1994, 2008) and España-Chamorro (2019).

This paper’s contribution to the debate is the archaeological identification of the *Ianus Augustus* and the road that runs through this significant landmark. In our opinion, the long biography and diachronic use of the studied road cannot correspond to the secondary road of the *Alio itinere*, but to a highly transited Imperial road such as the main route of the *Via Augusta*. In part, M.G. Schmidt argues his hypothesis based on the identification of the Roman town located in Cerro Maquiz (Mengíbar) not as *Illiturgi* but as *Ossigi*. However, our research project involving systematic excavation and extensive surveys in that region and settlement has led us to conclude that this site can in fact be identified as ancient *Illiturgi* (Fig. 1) (Bellón Ruiz et al. 2017a, b, 2021). As stated by España-Chamorro (2017, p. 20), the *Ianus Augustus* was the most important landmark in the road network of *Baetica* province, as can be seen from milestones such as the one identified in Cadix (CIL, II, 4734) that counts the miles from the *Ianus*, despite being 350 km away (Fig. 1). The fact that the milestones on the *Via Augusta* count the miles to and from the *Ianus* and not from other points in the provincial geography is very significant, especially considering that the provincial road network had a radial structure around the provincial and conventual capitals of *Corduba*, *Astigi*, *Hispalis* and *Gades* (España-Chamorro 2017; España Chamorro 2019) (Fig. 1). Now that the *Ianus* has been archaeologically identified and the road that passes through it runs parallel to the River Guadalquivir, as shown in excavation and the different analyses carried out in this study, in our opinion, it is difficult to state that this road is the *Alio itinere* and not the main route of the *Via Augusta*. This interpretation makes even more sense when considering the presence of several *mansiones* (state post offices) on the northern route, such as at *Ad Decumum*, *Ad Lucos* and *Ad Noulas* (Fig. 2A). We must also remind ourselves that *Baetica* province takes its name etymologically from the hydronym of the River Baetis (Guadalquivir), which played an important role in the birth and evolution of the town planning and structuring of the provincial landscape, as it was the main provincial communication axis, thanks to the fluvial connection, as well as the *Via Augusta*.

## Conclusions

The archaeological characterisation of *capita viarum* (the strategic starting points of the road network in the Roman Empire), such as the *Ianus Augustus*, allows us to understand

the territorial organisational dynamic on a macroscale, as well as the mobility, interprovincial communications and mental landscapes of ancient Roman travellers. In the case of the *Ianus Augustus*, this is especially important as this *caput viae* coincides with the *fines provincia* or interprovincial limit. The significance of this monument, however, was even more pronounced given that the *Via Augusta*, the main road of Roman *Hispania*, ran through it, connecting the Atlantic Ocean (the *fines imperium* or boundaries of the Empire) and *Baetica* province with Rome itself. Thus, this monument and the interprovincial border at this point made even more sense because of the presence of the *Via Augusta*. In this respect, in addition to its symbolic dimension, the *Ianus Augustus* played an important role in regulating and ensuring the rights of goods and people to pass between the provinces.

However, much information of this road was preserved at the microscale, where the application of microstratigraphic techniques of analysis allowed the identification of six overlying roads and their construction techniques in a biographic way. In addition to being very effective in unravelling the road sequence and characterising its deposits, microstratigraphic analysis have shown that the builders of this road used specific architectural and engineering knowledge with technical solutions adapted to the possibilities and limitations of the area. More studies of Roman roads from a geoarchaeological perspective are needed to make regional and supraregional comparisons of the building techniques, technical solutions and biographies of these prominent constructions that are omnipresent across the Roman Empire. This study offers one of the few characterisations of a Roman road on a microfacies scale and, due to the nature of the deposits composed of gravels, it enriches the corpus of features already described in the literature. Furthermore, the microstratigraphic analysis has provided significant new data of great historical value. Apart from contributing to identifying the layout of the *Via Augusta* on a regional level, our results show how the technical solutions, building techniques and general know-how of its builders survived as a tradition throughout the active life of the road, from its construction in the first century AD to the different repair works carried out at least until the fourth century AD, when the *Ianus Augustus* was systematically dismantled.

**Acknowledgements** The authors thank both anonymous reviewers for their comments on the original manuscript and their stimulating questions and suggestions. The authors wish to acknowledge the financial support provided by institutions involved in this research. The research team wishes to express its gratitude to Mengibar Town Council (Jaén), the Friends of the Iberians Association and the Institute of Iberian Archaeology (University of Jaén). Their collaboration and contributions made it possible to begin investigating the site. The authors also thank the Provincial Government, particularly to Narciso Zafra, specialist from the Territorial Department of Culture, for his support and contributions to the excavations. We would also like to thank Alfonso

Montejo for his work on drawing up the dossier for the declaration of the Arch of Augustus as an Asset of Cultural Interest. The archaeological investigations carried out in *Ianus Augusti* are included within the framework of the research project “Metodología para el estudio arqueológico de campos de batalla y asedios en el contexto de la Segunda Guerra Púnica: Metauro, Ilturgi y Cástulo (207/206 a.n.e)” (HAR2016-77847-P). This project is directed by J.P.B.R. and funded by the Ministry of Economy, Industry and Competitiveness of Spain. The University of Granada provided a postdoctoral grant to M.G.-R. in the School of Archaeology and Ancient History of University of Leicester (Programa de Perfeccionamiento de Doctores, Plan Propio del Vicerrectorado de Investigación). M.G.-R. thanks the support and funding received from the Juan de la Cierva-Formación Subprogramme (FJC2019-041335-I) funded by the Ministry of Science and Innovation of Spain (MCIN/AEI/10.13039/501100011033) and by the European Union (NextGenerationEU/PRTR). M.G.-R. thanks David Mattingly, Huw Barton, José C. Carvajal, Sarah Morriss and Danielle de Carle for their useful comments and the facilities provided in the XRF laboratory at the School of Archaeology and Ancient History (University of Leicester). We thank our colleagues Alberto Sánchez Vizcaíno (UIAI-University of Jaén) and José C. Cristóbal Carvajal (SAAH-University of Leicester) for their comments and suggestions on the manuscript.

**Funding** Open Access funding provided thanks to the CRUE-CSIC agreement with Springer Nature. Ministerio de Economía, Industria y Competitividad, Gobierno de España, HAR2016-77847-P, Juan Pedro Bellón Ruiz, Universidad de Granada, Programa 8. Perfeccionamiento de doctores. Plan Propio del Vicerrectorado de Investigación, Mario Gutiérrez-Rodríguez

## Declarations

**Conflict of interest** The authors declare no competing interests.

**Open Access** This article is licensed under a Creative Commons Attribution 4.0 International License, which permits use, sharing, adaptation, distribution and reproduction in any medium or format, as long as you give appropriate credit to the original author(s) and the source, provide a link to the Creative Commons licence, and indicate if changes were made. The images or other third party material in this article are included in the article's Creative Commons licence, unless indicated otherwise in a credit line to the material. If material is not included in the article's Creative Commons licence and your intended use is not permitted by statutory regulation or exceeds the permitted use, you will need to obtain permission directly from the copyright holder. To view a copy of this licence, visit <http://creativecommons.org/licenses/by/4.0/>.

## References

- Albenga G (1918) La evoluzione della strada – I. La strada antica. Tipografia editrice Cav. F. Mariotti, Pisa
- Ariño Gil E, Palet Martínez JM, Gurt Esparraguera JM (2004) El pasado presente. Ediciones Universidad de Salamanca, Salamanca, Arqueología de los paisajes en la Hispania Romana
- Baena R (1993) Evolución cuaternaria (3 M.a) de la Depresión del Medio-Bajo Guadalquivir y sus márgenes (Córdoba y Sevilla). Universidad de Sevilla
- Baltrusch E, Czeguhn I, Esders S, et al (2016) Infrastructures, mobility and water management. The Iberian Peninsula in the Imperial and Post-Imperial Context. *eTopoi Journal of Ancient Studies* 6. Space and Knowledge:220–249

- Batino S, Corradi L, Corradi M, et al (1999) Il traffico sull'antica via Flaminia: viabilità e mezzi di trasporto romani. Edizioni Thyrsus, Arrone
- Bellón Ruiz JP, Lechuga Chica MA, Moreno Padilla MI, Gutiérrez-Rodríguez M (2021) Ianus Augustus, Caput Viae (Mengibar, Spain): An interprovincial monumental border in Roman Hispania. *Journal of Roman Archaeology* 34:3–29. <https://doi.org/10.1017/S1047759421000283>
- Bellón Ruiz JP, Lechuga Chica MA, Rueda Galán C et al (2021) De situ Iiliturgi, análisis arqueológico de su asedio en el contexto de la Segunda Guerra Púnica. *Archivo Español de Arqueología* 94:e15
- Bellón Ruiz JP, Molinos Molinos M, Rueda Galán C, et al (2017a) Rome versus Carthage: the second Punic War battlefield of Baecula and the siege of Iiliturgi. In: Fernández-Götz M, Roymans N (eds) *Conflict archaeology. Materialities of Collective Violence from Prehistory to Late Antiquity*. European Association of Archaeologists. Routledge. Taylor and Francis Group, London
- Bellón Ruiz JP, Rueda Galán C, Lechuga Chica MA (2017b) Iiliturgi delenda est: arqueología de la Segunda Guerra Púnica. In: Masseria C, Marroni E (eds) *Dialogando. Studi in onore de Mario Torelli*. Edizioni ETS, Pisa, pp 19–30
- Berechman J (2003) Transportation—economic aspects of Roman highway development: the case of Via Appia. *Transportation Research Part a: Policy Practice* 37:453–478. [https://doi.org/10.1016/S0965-8564\(02\)00056-3](https://doi.org/10.1016/S0965-8564(02)00056-3)
- Bergier N (1622) *Histoire des grands chemins de l'empire romain*. Paris
- Bernardini F, Vinci G, Forte E et al (2018) Discovery of ancient Roman “highway” reveals geomorphic changes in karst environments during historic times. *PLoS ONE* 13:e0194939. <https://doi.org/10.1371/journal.pone.0194939>
- Bertran P, Teixier J-P (1999) Facies and microfacies of slope deposits. *CATENA* 35:99–121. [https://doi.org/10.1016/S0341-8162\(98\)00096-4](https://doi.org/10.1016/S0341-8162(98)00096-4)
- Blázquez A (1914) Vías romanas de Andalucía. Informe sobre una comunicación de D. Ángel Delgado. *Boletín De La Real Academia De La Historia* 64:525–533
- Botazzi G (1992) Le vie pubbliche centuriali tra Modena e Piacenza. In: Quilici L, Quilici S (eds) *Tecnica Stradale Romana*. L'Erma di Bretschneider, Roma, pp 169–178
- Cammass C, Watez J (2009) L'approche micromorphologique : méthode et applications aux stratigraphies archéologiques. In: Ferdière A (ed) *La géologie : les sciences de la Terre appliquées à l'Archéologie*. Errance, Paris, pp 181–216
- Capedri S, Grandi R, Venturelli G (2003) Trachytes used for paving Roman roads in the Po plain: characterization by petrographic and chemical parameters and provenance of flagstones. *J Archaeol Sci* 30:491–509. <https://doi.org/10.1006/jasc.2002.0857>
- Charbonnier M-C, Cammass C (2018) Characterization of Gallo-Roman roads in northern France using micromorphological methods. *Quatern Int* 483:194–210. <https://doi.org/10.1016/j.quaint.2018.05.010>
- Charbonnier M-C, Cammass C (2015) Apport de la géoarchéologie à l'étude des espaces de circulation dans les villes antiques (Nord de la France). *Revue Du Nord Hors-Série- Collection Art Et Archéologie* 13:133–146
- Chevalier P (1997) *Les Voies Romaines*. Picard, Paris
- Chouquer G, Favory F (1991) *Les paysages de l'Antiquité. Terres et cadastres de l'Occident romain*. Errance, Paris
- Ciampoltrini G, Andreotti A (1994) Vie rurali d'età romana nell'Ager Lucensis: contributi dell'alveo del Bientina. In: Quilici L, Quilici S (eds) *Strade romane: Percorsi e infrastrutture*. Atlante tematico di topografia antica. L'Erma di Bretschneider, Roma, pp 183–192
- Corzo Sánchez R, Toscano San Gil M (1992) *Las vías romanas de Andalucía*. Dirección General de Ordenación del Territorio. Junta de Andalucía, Sevilla
- Courty M-A (2001) Microfacies analysis assisting archaeological stratigraphy. In: Goldberg P, Holliday VT, Ferring CR (eds) *Earth sciences and archaeology*. Springer, US, Boston, MA, pp 205–239
- Courty M-A, Macphail RI, Goldberg P (1989) *Soils and micromorphology in archaeology*. Cambridge University Press, Cambridge
- España Chamorro S (2021) *Unde incipit Baetica*. Los límites de la Baetica y su integración territorial (s. I-III). L'Erma di Bretschneider, Roma
- España Chamorro S (2019) *Corpus Milliariorum Baeticae*. Miliarios y política viaria en la Hispania Ulterior Baetica en época imperial (s- I-IV). *Archeologia Classica* LXX:397–454
- España-Chamorro S (2017) Los capita viarum de la provincia Baetica. *Anales de Arqueología Cordobesa* 28:11–32. <https://doi.org/10.21071/aac.v28i0.10188>
- Evangelidis V, Tsompanas M-A, Sirakoulis GCh, Adamatzky A (2015) Slime mould imitates development of Roman roads in the Balkans. *J Archaeol Sci Rep* 2:264–281. <https://doi.org/10.1016/j.jasrep.2015.02.005>
- Flügel E (2004) *Microfacies of carbonate rocks: analysis, interpretation and application*. Springer-Verlag, Berlin, Heidelberg
- Forbes RJ (1964) Notes on the history of ancient roads and their construction. Adolf M. Hakkert, Amsterdam
- Franco-Sánchez F (2017) La toponimia árabe de los espacios viales y los espacios defensivos en la Península Ibérica. In: Carvalho C, Planelles Iváñez M, Sandakova E (eds) *De la langue à l'expression: le parcours de l'expérience discursive*. Hommage à Marina Aragón Cobo. Publicacions de la Universitat d'Alacant, Sant Vicent del Raspeig, pp 167–190
- Fustier P (1960) Notes sur la constitution des voies romaines en Italie. *Revue Des Études Anciennes* 62:95–99. <https://doi.org/10.3406/rea.1960.3641>
- Garilli E, Autelitano F, Giuliani F (2017) A study for the understanding of the Roman pavement design criteria. *J Cult Herit* 25:87–93. <https://doi.org/10.1016/j.culher.2017.01.002>
- Gasparini M, Moreno-Escribano JC, Monterroso-Checa A (2019) Identifying the Roman road from Corduba to Emerita in the Puente Nuevo reservoir (Espiel-Córdoba/Spain). *J Archaeol Sci Rep* 24:363–372. <https://doi.org/10.1016/j.jasrep.2019.01.026>
- Gautier H (1769) *Architettura delle strade antiche e moderne*. Antonio Veronese, Vicenza
- Gé T, Courty M-A, Matthews W, Watez J (1993) Sedimentary formation processes of occupation surfaces. In: Goldberg P, Nash DT, Petraglia MD (eds) *Formation processes in archaeological context*. Prehistory Press, pp 149–163
- Gebhardt A, Langohr R (2015) Traces de roulage ou de labour ? Le diagnostic micromorphologique. *ArcheoSciences Revue d'archéométrie* 31–38. <https://doi.org/10.4000/archeosciences.4363>
- Goldberg P, Miller CE, Schiegl S et al (2009) Bedding, hearths, and site maintenance in the Middle Stone Age of Sibudu Cave, KwaZulu-Natal, South Africa. *Archaeol Anthropol Sci* 1:95–122. <https://doi.org/10.1007/s12520-009-0008-1>
- González Tascón I, Velázquez Soriano I (2004) *Ingeniería romana en Hispania: historia y técnicas constructivas*. Fundación Juanolo Turriano, Madrid
- Guédon S (2018) *La frontière romaine de l'Africa sous le Haut-Empire*. Casa de Velázquez, Madrid
- Güimil-Fariña A, Parcero-Oubiña C (2015) “Dotting the joins”: a non-reconstructive use of least cost paths to approach ancient roads. The case of the Roman roads in the NW Iberian Peninsula. *J Archaeol Sci* 54:31–44. <https://doi.org/10.1016/j.jas.2014.11.030>
- Gutiérrez-Rodríguez M, Toscano M, Goldberg P (2018) High-resolution dynamic illustrations in soil micromorphology: a proposal for presenting and sharing primary research data in publication. *J Archaeol Sci Rep* 20:565–575. <https://doi.org/10.1016/j.jasrep.2018.05.025>

- Hitchner RB (2012) Roads, integration, connectivity, and economic performance in the Roman Empire. In: Highways, byways, and road systems in the pre-modern world. John Wiley & Sons, Ltd, pp 222–234
- Holland LA (1961) *Ianus and the bridge*. American Academy in Rome, Roma
- Hübner E (1888) *La Arqueología de España*. Madrid
- ITGE MAPA GEOLÓGICO DE ESPAÑA (1990a) E. 1:50.000 Hoja 926 MENGÍBAR. Segunda Serie. Primera edición. Instituto Tecnológico GeoMinero de España, Madrid
- ITGE MAPA GEOLÓGICO DE ESPAÑA (1990b) E. 1:50.000 Hoja 905 LINARES. Segunda Serie. Primera edición. Instituto Tecnológico GeoMinero de España, Madrid
- Jimenez-Espinosa R, Jimenez-Millán J, Garcia-Tortosa FJ (2016) Upper-Pleistocene terrace deposits in Mediterranean climate: geomorphological and source-rock control on mineral and geochemical signatures (Betic Cordillera, SE Spain). *J Iber Geol* 42:187–200. [https://doi.org/10.5209/rev\\_JIGE.2016.v42.n2.52865](https://doi.org/10.5209/rev_JIGE.2016.v42.n2.52865)
- Karkanas P, Goldberg P (2019) Reconstructing archaeological sites: understanding the geoarchaeological matrix. Wiley Blackwell
- Keay SJ, Parcak SH, Strutt KD (2014) High resolution space and ground-based remote sensing and implications for landscape archaeology: the case from Portus, Italy. *J Archaeol Sci* 52:277–292. <https://doi.org/10.1016/j.jas.2014.08.010>
- Kolb A (2019) *Roman roads. New evidence, new perspectives*. De Gruyter, Berlin, Boston
- Lorite-Herrera M, Jiménez-Espinosa R, Jiménez-Millán J, Hiscock KM (2008) Integrated hydrochemical assessment of the Quaternary alluvial aquifer of the Guadalquivir River, southern Spain. *Appl Geochem* 23:2040–2054. <https://doi.org/10.1016/j.apgeochem.2008.03.013>
- Magli G, Realini E, Reguzzoni M, Sampietro D (2014) Uncovering a masterpiece of Roman engineering: the project of Via Appia between Colle Pardo and Terracina. *J Cult Herit* 15:665–669. <https://doi.org/10.1016/j.culher.2013.11.014>
- Melchor Gil E (1994) Comunicaciones terrestres entre Corduba y Castulo: su problemática. In: II Congreso de Historia de Andalucía. Historia Antigua. Junta de Andalucía. Consejería de Cultura y Medio Ambiente, Córdoba, pp 453–468
- Melchor Gil E (2008) El Baetis y la organización viaria del sur peninsular: la interconexión de las redes de transporte fluvial y terrestre en la Bética romana. *Anas* 21–22:163–191
- Moreno Gallo I (2004) *Vías romanas. Ingeniería y técnica constructiva*. Ministerio de Fomento. Centro de Estudios Históricos de Obras Públicas (CEHOPU)
- Nemec W, Steel RJ (1984) Alluvial and coastal conglomerates: their significant features and some comments on gravelly mass-flow deposits. In: Koster EH, Steel RJ (eds) *Sedimentology of Gravels and Conglomerates*. Canadian Society of Petroleum Geologists, Calgary, pp 1–31
- Orengo HA, Livarda A (2016) The seeds of commerce: a network analysis-based approach to the Romano-British transport system. *J Archaeol Sci* 66:21–35. <https://doi.org/10.1016/j.jas.2015.12.003>
- Petrucci E (2013) *Renovatio pavimentorum. Metodologie d'intervento per le antiche pavimentazioni stradali*. Franco Angeli, Milano
- Quilici L (1992) Evoluzione della tecnica stradale nell'Italia centrale. In: Quilici L, Quilici S (eds) *Tecnica Stradale Romana. L'Erma di Bretschneider*, Roma, pp 19–32
- Quilici L, Quilici S (eds) (1992) *Tecnica Stradale Romana. L'Erma di Bretschneider*, Roma
- Radke G (1981) *Viae Publicae Romanae – Traduzione di Gino Sigismondi*. Nuova casa editrice Cappelli, Bologna
- Rentzel P, Nicosia C, Gebhardt A, et al (2017) Trampling, poaching and the effect of traffic. In: Nicosia C, Stoops G (eds) *Archaeological soil and sediment micromorphology*. John Wiley & Sons, Ltd, pp 281–297
- Rodríguez Morales J (2011) Calzadas romanas, ¿Propaganda o utilidad? In: Bravo G, González Salinero R (eds) *Propaganda y persuasión en el mundo romano. Actas del VIII Coloquio de la Asociación Interdisciplinar de Estudios Romanos, celebrado en Madrid los días 1 y 2 de diciembre de 2010*. Signifer Libros, Madrid, pp 177–212
- Rodríguez Morales J (2010) Las vías romanas en la erudición moderna. Reivindicación de Nicolás Bergier. In: Moreno Gallo I (ed) *Las técnicas constructivas en la ingeniería romana. Actas del V congreso de las obras públicas romanas*. pp 119–134
- Roduit N (2007) *JMicroVision: un logiciel d'analyse d'images pétrographiques polyvalent*. Université de Genève
- Roldán Hervás JM (1975) *Itineraria hispana: fuentes antiguas para el estudio de las vías romanas en la Península ibérica*. Departamento de Historia Antigua, Universidad de Granada, Granada, Departamento de Historia Antigua, Universidad de Valladolid
- Roldán Hervás JM, Caballero Casado C (2014) *Itinera Hispana. Estudio de las vías romanas en Hispania a partir del Itinerario de Antonino, el Anónimo de Ravena y los Vasos de Vicarello*. undación Juanelo Turriano, Consejería de Educación y Cultura del Gobierno de Extremadura, Colegio de Ingenieros de Caminos, Canales y Puertos, Madrid
- Rosada G (1992) *Tecnica stradale e paesaggio della decima regio*. In: Quilici L, Quilici S (eds) *Tecnica Stradale Romana. L'Erma di Bretschneider*, Roma, pp 39–50
- Schattner T, Ruipérez H (2010) Entradas a ciudades romanas de Hispania: el ejemplo de Córdoba. In: Vaquerizo D (ed) *Las áreas suburbanas en la ciudad histórica : topografía, usos, función*. Universidad de Córdoba, Córdoba, pp 95–116
- Schmidt MG (2013) Roads and towns along the border of Hispania Citerior. In: López Vilar J (ed) *Tarraco biennial 1er Congrès international d'archéologie i món antic: Govern i societat a la Hispania romana, novetats epigràfiques. Homenatge a Géza Alföldy*. Fundació Privada Mútua Catalana, Tarragona, pp 291–299
- Schmidt MG (2018) “Ab Iano Augusto ad Oceanum”. *Methodologische Überlegungen zur Erforschung der viae publicae in der Baetica*. In: Czeguhn I, Möller C, Quesada Y, Pérez JA (eds) *Wasser - Wege - Wissen auf der iberischen Halbinsel Eine interdisziplinäre Annäherung im Verlauf der Geschichte*. Nomos Verlag, Baden-Baden, pp 35–53
- Sidebotham SE, Zitterkopf RE, Helms CC (2000) Survey of the Via Hadriana: the 1998 season. *Journal of the American Research Center in Egypt* 37:115–126. <https://doi.org/10.2307/40000526>
- Sillières P (1990) *Les voies de communication de l'Hispanie méridionale*. Boccard, Paris
- Sillières P (1981) À propos d'un nouveau milliaire de la Via Augusta, une via militaris en Bétique. *Revue Des Études Anciennes* 83:255–271. <https://doi.org/10.3406/rea.1981.4114>
- Sillières P (1994) *Le Ianus Augustus*. In: Bedon R, Martin PM (eds) *Mélanges Raymond Chevallier. Vol. 2: Histoire et archéologie*. pp 305–311
- Sillières P (1976) *La Via Augusta de Cordoue à Cadix. Documents du XVIII s. et photographies aériennes pour une étude de topographie historique*. Mélanges De La Casa De Velázquez 12:27–67
- Stoops G (2003) Guidelines for analysis and description of soil and regolith thin sections. Soil Science Society of America Inc., Madison, Wisconsin, USA
- Stoops G, Marcelino V, Mees F (eds) (2010) *Interpretation of micromorphological features of soils and regoliths*. Elsevier, Amsterdam
- Stoops G, Mees F (2018) Chapter 5 - groundmass composition and fabric. In: Stoops G, Marcelino V, Mees F (eds) *Interpretation of micromorphological features of soils and regoliths (Second Edition)*. Elsevier, pp 73–125

- Torres Balbás L (1959) La vía Augusta y el arrecife musulmán. *Al-Andalus* XXIV:441–448
- Ventura Villanueva A (2013) Inscripción del emperador Claudio, alusiva a la restauración de la Vía Augusta, en Bujalance. *Adalid* 4:77–85
- Verbrugge G, De Clercq W, Van Eetvelde V (2017) Routes across the Civitas Menapiorum: using least cost paths and GIS to locate the Roman roads of Sandy Flanders. *J Hist Geogr* 57:76–88. <https://doi.org/10.1016/j.jhg.2017.06.006>
- Wouters B (2020) A biographical approach to urban communities from a geoarchaeological perspective: high-definition applications and case studies. *J Urban Archaeol* 2:85–101. <https://doi.org/10.1484/J.JUA.5.121530>
- Xeidakis GS, Varagouli EG (1997) Design and construction of roman roads: the case of Via Egnatia in the Aegean Thrace, Northern Greece. *Environ Eng Geosci* III:123–132. <https://doi.org/10.2113/gseegeosci.III.1.123>
- Zanón J (1986) Un itinerario de Córdoba a Zaragoza en el siglo X. *Al-Qantara Revista De Estudios Árabes* 7:31–52

**Publisher's note** Springer Nature remains neutral with regard to jurisdictional claims in published maps and institutional affiliations.